Journal of South American Earth Sciences 73 (2017) 100–118

Contents lists available at ScienceDirect

Journal of South American Earth Sciences

journal homepage: www.elsevier.com/locate/jsames

La Escalerilla pluton, San Luis Argentina: The orogenic and post-orogenic magmatic evolution of the famatinian cycle at Sierras de San Luis

Augusto Francisco Morosini [a, c, *], Ariel Emilio Ortiz Suárez [a], Juan Enrique Otamendi [b, c], Diego Sebastián Pagano [a, c], Gabriel Alejandro Ramos [a]

[a] Departamento de Geología, Universidad Nacional de San Luis, 5700, San Luis, Argentina
[b] Departamento de Geología, Universidad Nacional de Río Cuarto, 5800, Río Cuarto, Argentina
[c] Consejo Nacional de Investigaciones Científicas y Técnicas (CONICET), Argentina

ARTICLE INFO

Article history:
Received 22 July 2016
Received in revised form
1 November 2016
Accepted 1 December 2016
Available online 2 December 2016

Keywords:
La Escalerilla pluton
El Volcán pluton
Geochronology
Geochemical contrast
Sierra de San Luis
Famatinian orogeny

ABSTRACT

Field relationships, geochemical analysis and two new absolute ages (LA-MC-ICP-MS U/Pb-zircon) allow the division of the La Escalerilla pluton (previously considered to be a single granitic body) into two different plutons: a new La Escalerilla pluton (s.s.), dated at 476.7 ± 9.6 Ma, that represents the northern portion, and the El Volcán pluton, dated at 404.5 ± 8.5 Ma, located in the southern sector. The La Escalerilla pluton is composed of three facies: (1) biotite-bearing granodiorite, (2) porphyritic biotite-bearing granite, and (3) porphyritic two micas-bearing leucogranite, being the presence of late-magmatic dykes in these facies common. The El Volcán pluton is composed of two main facies: 1) porphyritic biotite-bearing granite, and 2) two micas-bearing leucogranite, but amphibole-bearing monzodioritic and tonalititic mega-enclaves are also common, as well as some dykes of amphibole and clinopyroxene-bearing syenites. A peculiarity between the two plutons is that their most representative facies (porphyritic biotite-bearing granites) have, apart from different absolute ages, distinctive geochemical characteristics in their concentrations of trace elements; the La Escalerilla granite is comparatively poorer in Ba, Sr, Nb, La, Ce, P, and richer in Rb, Tb, Y, Tm and Yb. The El Volcán granite is notably enriched in Sr and depleted in Y, resulting in high Sr/Y ratios (12.67–39.08) compared to the La Escalerilla granite (1.11–2.41). These contrasts indicate that the separation from their sources occurred at different depths: below 25 km for the La Escalerilla, and above 30 km for the El Volcán. Moreover, the contrasts allow us to interpret a thin crust linked to an environment of pre-collisional subduction for the first case, and a thickened crust of post-collisional environment for the second, respectively.

© 2016 Elsevier Ltd. All rights reserved.

1. Introduction

The magmatic evolution of the southwestern sector of the Sierra de San Luis has been the focus of investigation for the last 15 years (e.g.: Ortiz Suárez et al., 1992; Sato et al., 1996, 2003a, 2003b; Sims et al., 1998; von Gosen, 1998; von Gosen et al., 2002; Llambías et al., 1998; González et al., 2002; Brogioni et al., 2005; López de Luchi et al., 2002, 2007; Steenken et al., 2006, 2008; Morosini et al., 2009; Morosini, 2011, and others).

One of the main and most representative examples of this magmatism is the La Escalerilla pluton (LEP). This plutonic body has opened a debate as to its temporary location, since it has been considered to be part of the pre-orogenic Ordovician plutonic age (Ortiz Suárez et al., 1992; Sato et al., 1996; Llambías et al., 1998; von Gosen et al., 2002; Brogioni et al., 2005), as well as part of the post-orogenic Devonian plutonic age (Sims et al., 1998; López de Luchi et al., 2002; 2007; Steenken et al., 2006, 2008). However, new questions have arisen since the work of von Gosen et al. (2002), who determined a new age of 507 ± 24 Ma for the north of the LEP, showing great difference from the age (403 ± 6 Ma) proposed by Sims et al. (1998) for the southern sector. Based on these ages von Gosen et al. (2002) proposed a Devonian pluton in the southern sector, which was called El Volcán, whose limit (inferred) with the

* Corresponding author. Departamento de Geología, Universidad Nacional de San Luis, 5700, San Luis, Argentina.
E-mail address: afmorosini@gmail.com (A.F. Morosini).

http://dx.doi.org/10.1016/j.jsames.2016.12.001
0895-9811/© 2016 Elsevier Ltd. All rights reserved.

La Escalerilla pluton would be an intrusive contact (Fig. 2; von Gosen et al., 2002).

In this paper, through a series of detailed analyses of field relationships, the petrography of the plutons, whole-rock compositions data and two new U-Pb zircon ages, we demonstrate that: 1) LEP is a composite pluton, built by several intrusions of different magmas and 2) there are different ages between the central-north and the southern areas, which according to von Gosen et al. (2002) makes it possible to assign a new pluton in the southern sector, El Volcán pluton (EVP), with distinctive characteristics and a younger age. Finally, taking into account published and new data we contribute to the understanding of the geodynamic context where these specific plutons were generated and emplaced.

2. Methodology

This paper results from intense work of field based on the petrological and structural analysis. The cartography was done with ASTER images and a satellite image obtained with the Stitch Maps software from Google Earth. Thin sections were petrographically described and modal compositions were obtained with a manual point counter using 1000 points per thin section. The classification of the rocks was based on the IUGS diagram (Le Maitre, 2002), and abbreviations for names of rock-forming minerals proposed by Whitney and Evans (2010) were used. Whole-rock analyses were performed by Activation Laboratories at Ancaster, Ontario (Canada). Rock powders were fused using a mixture of Li meta and tetraborate, dissolved in nitric acid and then analyzed by ICP-OES and ICP-MS.

Two absolute ages were determined by LA-MC-ICP-MS U/Pb-zircon method from both porphyritic biotite-bearing granites facies, one corresponding to the LE-g facies (sample O22), located in the inflexion zone of La Escalerilla pluton (S33°2′17″ - W66°10′26″), and the other corresponding to the EV-g facies (sample AA13), located in the southern sector of the area, within the El Volcán pluton (S33°12′5″ - W66°14′50″).

Zircon concentration was performed at the technical laboratory of the Geology Department of the Universidad Nacional de San Luis, and they were optically observed under petrographic and electron microscopy; backscattered electron images of the zircons were obtained in a *Scanning Electronic Microscope LEO 1450VP* (LABMEM - Universidad Nacional de San Luis).

Mounting and analysis of zircons were conducted at Laser Chron Center (University of Arizona, USA). Analytical conditions are equivalent to those reported by Ducea et al. (2010); a probe *New Wave/Lambda Physik DUV193 Excimer laser* (operating at a wavelength of 193 nm) was used, with a spot diameter of ~30 μm. All measurements were made in static mode, using Faraday detectors for ^{238}U and ^{232}Th, an ion-counting channel for ^{204}Pb, and either Faraday collectors or ion counting channels for $^{208-206}Pb$. Ion yield was ~1 mV ppm^{-1}. Each analysis consisted of a 20^{-s} integration on peaks with the laser off (for backgrounds), 20 1^{-s} integrations with the laser firing, and a 30^{-s} delay to purge the previous sample and prepare for the following analysis. The ablation pit was ~15 μm in depth. For each analysis, the errors in determining $^{206}Pb/^{238}U$ and $^{206}Pb/^{204}Pb$ resulted in a measurement error of ~1% (at 2σ level) in the $^{206}Pb/^{238}U$ age. The errors in measurement of $^{206}Pb/^{207}Pb$ and $^{206}Pb/^{204}Pb$ resulted in >1% (2σ) uncertainty in age, due to low intensity of the ^{207}Pb signal. Furthermore, common Pb correction was accomplished using the measurement of ^{204}Pb and assuming an initial Pb composition according to Stacey and Kramers (1975) (with uncertainty of 1.0 for $^{206}Pb/^{204}Pb$ and 0.3 for $^{207}Pb/^{204}Pb$). Uncertainty results obtained by calibration correction are generally ~1% (2σ) for both $^{206}Pb/^{238}U$ and $^{206}Pb/^{207}Pb$ ages. The uncertainties of the ages obtained for each sample are based on the scatter and precision of the whole set of $^{206}Pb/^{238}U$ and $^{206}Pb/^{207}Pb$ ages, weighted according to their measurement errors (shown at 1σ). The systematic error, which includes the standard calibration, standard calibration of age, and normal composition of Pb and U decay constants is generally ~1–2% (2σ).

We prefer to use conventional concordia diagrams because between $^{206}Pb/^{238}U$ and $^{207}Pb/^{235}U$ apparent ages are the best concordances, and the $^{206}Pb/^{207}Pb$ ages have the greatest uncertainties. In addition, we report as the final crystallization age for each sample the mean of the $^{206}Pb/^{238}U$ apparent values with highest concordance. Moreover, overlapping of analysis was carried by means of *Isoplot/Excel* (Ludwig, 2003).

3. Geological setting

The Sierra de San Luis belongs to the austral sector of the geological province of Sierras Pampeanas Orientales (Caminos, 1979), with a general NE-SW trend, approximately 160 km long and 80 km wide. It is composed of metamorphic and igneous rocks that belong to a debated evolution of Proterozoic-Paleozoic age which records the events that occurred in the Pampean, Famatinian and Achalian orogenic cycles. The Pampean Orogeny (Aceñolaza and Toselli, 1976; Dalla Salda, 1987; Rapela et al., 1992) has been interpreted by three hypotheses: (a) collision of an active seismic ridge against the Río de La Plata craton (Gromet and Simpson, 2000), (b) collision of a ridge against Kalahari craton and subsequent displacement by a transform fault to the Río de la Plata craton (Rapela et al., 2007), or (c) collision of an island arc with the Río de La Plata craton and subsequent Pampia terrain collision (Escayola et al., 2007; Ramos et al., 2014, and references therein). In either case, this orogeny develops from the Ediacaran to Stage 5 of the Cambrian, with a metamorphic climax at ~530 Ma. The Famatinian orogen is interpreted as a magmatic arc which was closed due to a collision caused by the interaction of an allochthonous terrane (Cuyania/Precordillera) derived from Laurentia (Thomas and Astini, 1996) on the western edge of Gondwana (Aceñolaza and Toselli, 1981; Rapela et al., 2001; Otamendi et al., 2009; Steenken et al., 2010), developed during Ordovician and Silurian periods. The Achalian orogeny corresponds to an intra-plate plutonic activity that occurred in the Devonian period (Sims et al., 1998; Stuart-Smith et al., 1999; López de Luchi et al., 2007).

The current north-south trending configuration of the Sierra de San Luis is the result of Andean tectonic compression processes (Jordan and Allmendinger, 1986; Ramos et al., 2002).

During the last three decades a large number of studies have focused on the structural evolution, metamorphism and magmatism of the basement in the Sierra de San Luis (Kilmurray and Dalla Salda, 1979; López de Luchi, 1987; Ortiz Suárez et al., 1992; Llambías et al., 1998; Sims et al., 1998; von Gosen and Prozzi, 1998; Delpino et al., 2001, 2007; González et al., 2002; Sato et al., 2003a, 2003b; López de Luchi et al., 2007; Steenken et al., 2006, 2008, 2010, 2011; Drobe et al., 2009; Morosini et al., 2009; Morosini and Ortiz Suárez, 2010, 2011).

The sierra is dominated by metamorphic rocks of different grades, of Precambrian-Early Paleozoic age, and intruded in the Paleozoic by different cycles of granitic plutonism (Gordillo and Lencinas, 1979; Ortiz Suárez et al., 1992; Llambías et al., 1998; Sato et al., 2003a; López de Luchi et al., 2007).

The metamorphic basement of the south of the Sierra de San Luis consists of three main NNE trending complexes (Fig. 1): Nogoli (NMC), Pringles (PMC), and Conlara (CMC) Metamorphic Complexes (Sims et al., 1998). These units are separated by two narrow low-grade belts of the San Luis Formation (SLF) which is described by Prozzi and Ramos (1988). Two names have been used to label different zones in the northern part of the Sierra de San Luis: Las

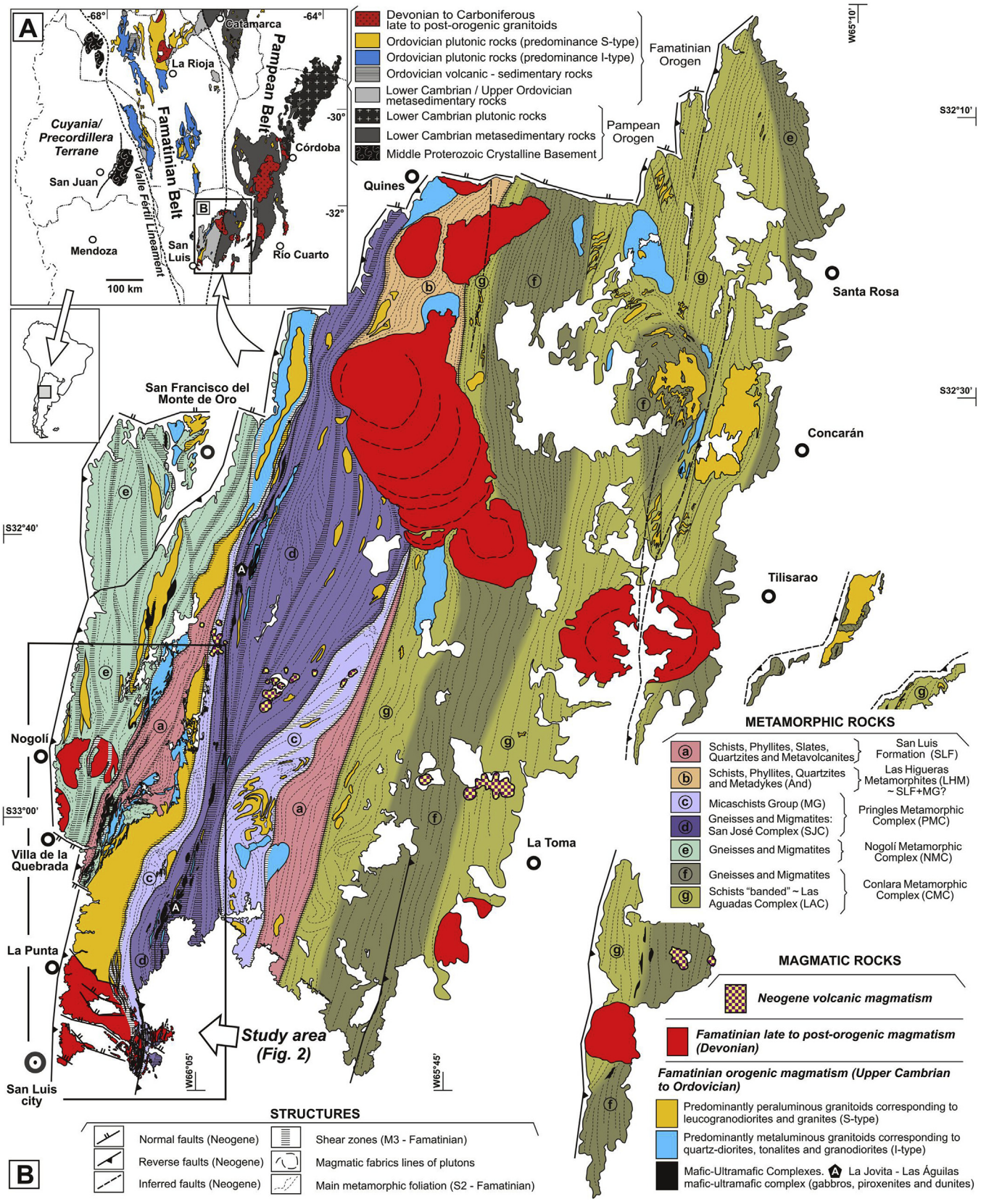

Fig. 1. (A) Map showing the location of the Sierra de San Luis with respect to the Pampean orogen, Famatinian magmatic arc, and Cuyania and/or Precordillera terrane. (B) Geological map of the Sierra de San Luis showing the distribution of metamorphic and plutonic units (modified from Sims et al., 1998; Ortiz Suárez, 1999; von Gosen et al., 2002; Sato et al., 2003a; Morosini, 2011; and others). The black box represents the location of the study area (Fig. 2).

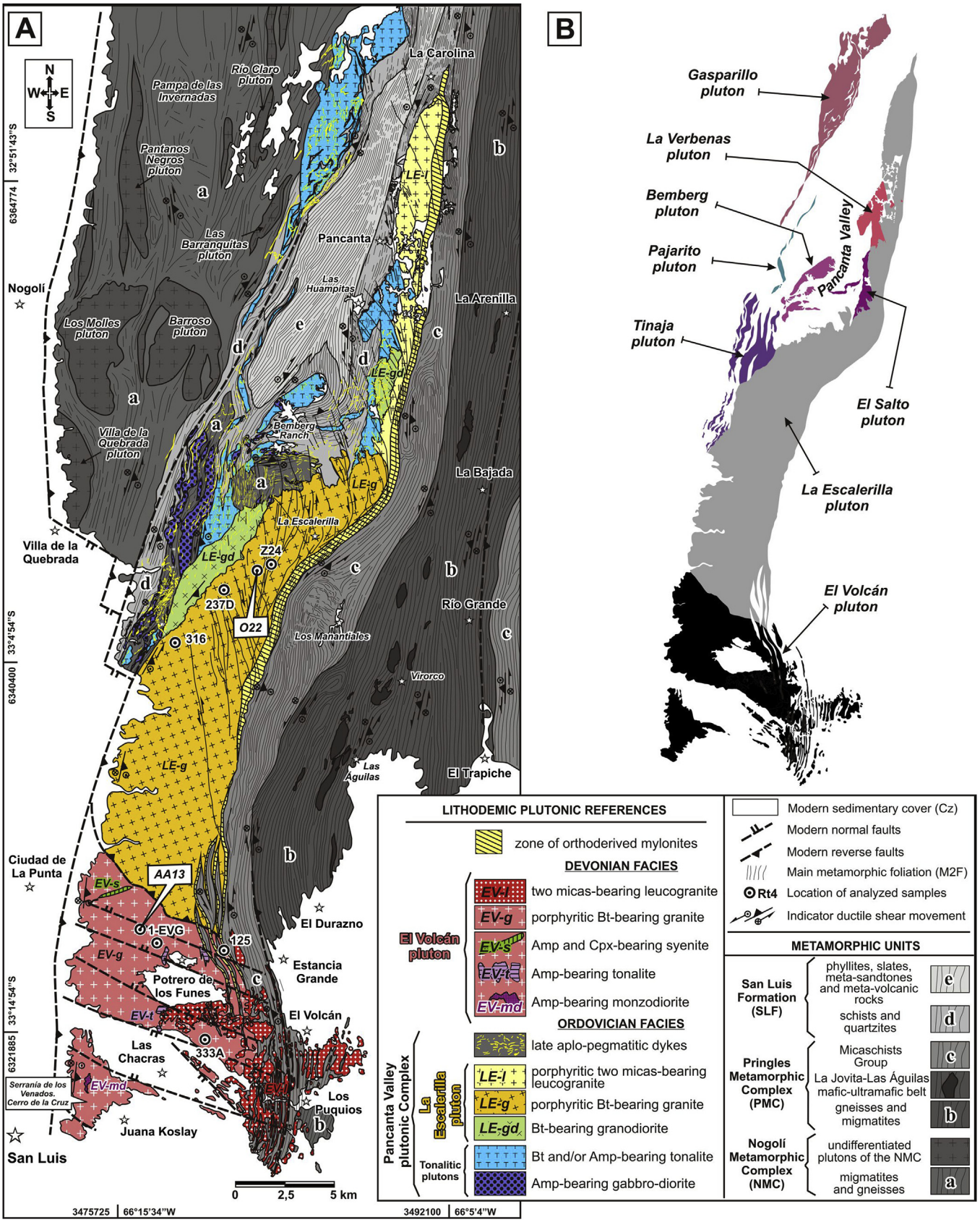

Fig. 2. (A) Geological map of the studied intrusive units, with location of the analyzed samples. (B) Distribution and names of the plutons.

Aguadas Complex (LAC, Ortiz Suárez, 1988) and Las Higueras Metamorphites (LHM, Grosso Cepparo et al., 2007). The LAC would be a middle-grade metamorphic zone within the CMC, while the features of LHM appear to be linked to the PMC and SLF. Nonetheless, the position and nature of the boundaries between the southern and northern metamorphic units are still unsolved and are a matter of study.

All the metamorphic rocks show a sub-vertical penetrative striking NNE foliation, which is attributed to the compression of Famatinian orogeny (Ortiz Suárez et al., 1992). This deformation in the middle to high-grade rocks developed on remnants of previous metamorphic structures (Sato et al., 2003a), which were considered pre-Famatinian (von Gosen and Prozzi, 1998; González, 2003; Sato et al., 2003a) and attributed to the Pampean orogeny (Kilmurray and Dalla Salda, 1979; Criado Roque et al., 1981).

Contacts between the metamorphic complexes of the Sierra de San Luis have a tectonic component, due to the development of ductile shear zones parallel to sub-parallel to the main famatinian metamorphic surface (NNE), which have favored the superposition of high-grade metamorphic complexes over those of low-grade, resulting in a metamorphic inversion (Ortiz Suárez and Casquet, 2005; Morosini et al., 2014). The observation of some transitional passages between metamorphic units of middle and low-grade (von Gosen and Prozzi, 1998; Sato et al., 2003a) has been less common.

The magmatism of the Sierra de San Luis is characterized by the presence of mafic-ultramafic rocks and a large number of granitoids of intermediate to acidic compositions.

Four mafic-ultramafic rocks groups were recognized, and they are the following: (1) La Jovita – Las Águilas (Kilmurray and Villar, 1981; Sato et al., 2003a; Cruciani et al., 2011, and references therein), (2) San Francisco – Villa de la Quebrada (Sato et al., 2003a, and references therein), (3) Las Cañas (Ortiz Suárez et al., 2012, and references therein) and (4) El Morro (Delakowitz et al., 1991).

Moreover, the bodies of granitoids rocks of the Sierra de San Luis have been classified as: (1) pre-kinematic, syn-kinematic and post-kinematic intrusives (Ortiz Suárez et al., 1992), with reference to the climax of the Famatinian orogeny which took place between 480 and 445 Ma, and based on the main geological features such as internal deformation, shaped bodies and rheological contrasts with the metamorphic host rocks; (2) Famatinian early pre-orogenic, Famatinian syn-orogenic, and Famatinian late to post-orogenic intrusives (Sato et al., 2003a). These authors distinguish within the pre-orogenic granitoids two groups, one of tonalite-granodiorite and one from granite-leucogranodiorites; and (3) two suites of Ordovician age and two suites of Devonian age (López de Luchi et al., 2007), the first two named Ordovician tonalite suite (OTS) and Ordovician granodiorite-granite suite (OGGS), both considered to be part of the Famatinian orogenic cycle, and the other two named Devonian granite suite (DGS) and Devonian monzonite-granite suites (DMGS), considered to be part of the Achalian orogenic cycle proposed by Sims et al. (1998). All these suites are syn-kinematic and are distinguished based on their main geochemical characteristics.

In this paper we refer to the set of granitoids of Upper Cambrian-Ordovician age of the Sierra de San Luis as Famatinian "orogenic" granitoids (considering a syn-metamorphic magmatism), and we solely make one distinction to separate a group having intermediate compositions, represented mainly by metaluminous to slightly peraluminous tonalite (I-type), from another of acid composition, represented by peraluminous to peraluminous felsic granites and leucogranodiorites (S-type), whose characteristics are equivalent to those reported by other authors (Llambías et al., 1998; Brogioni et al., 2005; López de Luchi et al., 2007). Furthermore, we will continue referring to the Famatinian post-orogenic granitoids when we mention the Devonian plutons. In this sense we consider the Achalian cycle proposed by Sims et al. (1998) as an ascent and erosions stage, as well as part of the Famatinian orogenic collapse (Fig. 1).

3.1. Host rock geology of the studied plutons

The regional metamorphic rocks hosting the LEP correspond to Nogolí Metamorphic Complex, Pringles Metamorphic Complex and San Luis Formation, but this pluton also intrudes tonalitic rocks of Las Verbenas, El Salto, and Tinaja plutons (Morosini, 2011, Fig. 2). On the other hand, for the EVP it is only possible to recognize Pringles Metamorphic Complex as metamorphic host-rock toward east, due to the absence of basement toward the south and west of the pluton, because this is covered by Neogene sediments; whereas that northward the host rocks of the EVP correspond to the LEP (Fig. 2). A summary of the main petrological characteristics of metamorphic host rocks and the relationship with the studied plutons is provided in Table 1.

4. Results

4.1. Geology and petrology of the plutons

For a better understanding of the geology and petrography of the studied plutons, hereinafter we do not refer to the LEP (s.l.) in a general term, rather we refer to the LEP in a strict sense (s.s.) for those rocks cropping out in the central and northern areas, and the EVP when we refer to the plutonic rocks that were previously considered to be the southern portion of the LEP (s.l.) (Fig. 2).

4.1.1. La Escalerilla pluton (LEP)

The LEP is a zoned elongated intrusive of 45 km long, which extends along the central and austral portion of the Paleozoic crystalline basement of the Sierra de San Luis, from La Carolina, in the north, to Potrero de los Funes locality, in the south (Fig. 2). The granitic massif reaches up to 6 km in width in its southern sector, but gradually becomes thinner northward, and exhibits a clear inflexion zone (homoclinal) in its central area (Figs. 1 and 2). The LEP is composed of three facies: (1) biotite-bearing granodiorite facies (LE-gd), (2) porphyritic biotite-bearing granite facies (LE-g), and (3) porphyritic two micas-bearing leucogranite facies (LE-l) (Fig. 3). There is also a swarm of aplo-pegmatitic granite dykes, cropping out both inside and outside the pluton (these are not described in the present paper).

4.1.1.1. Biotite-bearing granodiorite facies (LE-gd). The LE-gd facies is located in two sectors of the pluton, one with band-like form located in the western part of the inflexion zone (south of Bemberg Ranch), and another located further north. The contact between LE-gd and LE-g facies (as presented herein below) in the western part of the inflexion zone is transitional, due to a progressive increase in the size and concentration of K-feldspar phenocrysts. However, there are sites with inter-facies shear bands (~10 m).

The LE-gd facies exhibit high content of mafic microgranular enclaves (~5–80 cm) of dioritic and/or tonalitic composition, generally oriented following the internal magmatic fabric, and schlieren fabrics are common. Locally leucocratic syn-magmatic dykes of different thickness were recognized (Fig. 4A). The LE-gd facies has leuco-mesocratic color index (CI: 15-35) and shows equigranular medium-grained texture with a slightly foliated fabric. The rock consists of quartz, plagioclase (andesine: An_{43-50}), K-feldspar (microcline), and biotite (annite-phlogopite series), and as accessories zircon, sphene and allanite. Secondary minerals are represented by clinozoisite-epidote series and muscovite (Table 2). Quartz

Table 1
Main host rocks features; relationship between different host rocks and plutonic units in the study area.

	Lithologies	Metamorphism	Structures and fabric	Contact with La Escalerilla pluton			Contact with El Volcán pluton	
				Contact with LE-gd facies	Contact with LE-g facies	Contact with LE-l facies	Contact with EV-g facies	Contact with EV-l facies
Nogolí Metamorphic Complex	Paragneiss, orthogneiss, metatexites, diatexites, amphibolites	*High-grade* (high-amphibolite facies, Barrovian-type)	NNE to E axial planes of folded stromatic migmatites; nebulitic and schlieren; interference figures; siniestral-reverse mylonitic shear zones	Decoupled in the inflection zone and moderately coupled southwestward	Strongly decoupled in the inflection zone (stopping: offshoots with polygonal boundaries and dykes injected); moderately coupled southwestward (mylonitic boundary)	No contact	No contact	No contact
Micaschist Group (medium-grade of Pringles Metamorphic Complex)	Micaceous schists, quartz-feldspar schist, quartzites, calc-silicate, pegmatites	*Medium-grade* (from medium-greenschists to low-amphibolite facies, Barrovian-type)	NNE axial plane foliation; strong no-coaxial deformation siniestral-reverse mylonitic shear bands: lozenges, asymmetrical folds, pegmatitic boudins, interference figures, sigma-delta indicators)	No contact	Quite coupled, with a concordant siniestral-reverse mylonitic belt formed in the boundary	Quite coupled, with a concordant siniestral-reverse mylonitic belt formed in the boundary	Quite decoupled; the boundary is deformed and the host rock is accommodated following the shape of pluton	Strongly decoupled (stopping and injection), sometimes foliation planes are open by dikes, but in many cases they cut transversely
San Luis Formation	Phyllites, meta-sandstones, meta-conglomerates, micaceous schists, quartzites, meta-volcanites	*Low-grade* (from low- to medium-greenschists facies, Barrovian-type)	NNE axial plane folding (tight to isoclinal); near plutons there are shear bands with asymmetrical folds, boudins and echelon veins	No contact	Partially decoupled; boundary ductilely deformed and host rock curved following the shape of convergent lobes, which are associated with the magma advancing front, but in the end, they cut it; a thermal aureole is generated	Partially decoupled; the boundary is moderadely curve, greissen alteration and veins with wolfram-mineralization are present, they generated in conjugate echelon arrays system in the last stage post-cristallyzation (brittle-ductile transition of the host rock)	No contact	No contact
Tonalitic plutons previously intruded	leucotonatites, melatonalites, dioritic-gabbric enclaves, syn-magmatic leucocratic dykes	Partial recrystallization in subsolidus deformation (medium-greenschists facies)	Partially oblitered magmatic fabric; microgranular enclaves (mingling with gabbro-dioritic cogenetic magma); development of mylonites (S-C′ domains)	Partially decoupled magmatic contact; crushing of tonalite bodies by LE-gd facies in muhs stage (deformed acid dyke injections); in some sides they are mixing	Quite decoupled; intrusive contact (hectometrical irregular lobules of LE-g facies converging over tonalites, also subhorizontal dyke injections)	Strongly decoupled; intrusive tectonic contact; stopping (folieded tonalitic roof pendant are present)	No contact	No contact

For more detailed petrographic descriptions of the different metamorphic complex and tonalitic plutons see (e.g.: Sato et al., 1996; Llambías et al., 1998; Sims et al., 1998; von Gosen and Prozzi, 1998; Sato et al., 2003a; Brogioni et al., 2005; López de Luchi et al., 2007; Drobe et al., 2009; Steenken et al., 2010; Morosini, 2011).

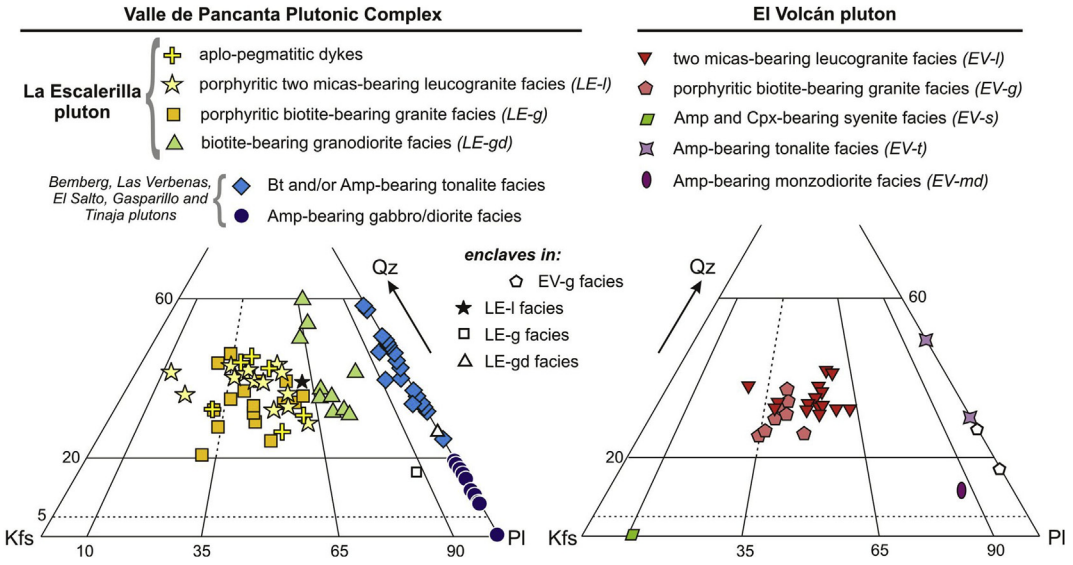

Fig. 3. QAP modal classification diagrams for the studied granitoids. The tonalitic and gabbro-dioritic facies partly correspond to plutons that are host rocks of LEP.

Fig. 4. Photographs corresponding to the outcrop and thin sections of La Escalerilla pluton. (A) Biotite-bearing granodiorite facies (LE-gd) with a leucocratic syn-magmatic dike. (B) Photomicrography of LE-gd facies; notice that K-feldespar is not present as phenocrysts. (C) Texture of the porphyritic biotite-bearing granite facies (LE-g); in the center of the photograph a K-feldespar fenocristal partially reabsorbed by the matrix. (D). Photomicrography of LE-g facies; zircon crystal with a core and edge representing two different stages of growth (this is probably an inherited core). (E) Texture of the porphyritic two micas-bearing leucogranite facies (LE-l); the color index is lower than in the LE-g facies. (F) Photomicrography of LE-l facies; the abundance of muscovite and the development of myrmekites are common in this rock. (For interpretation of the references to colour in this figure legend, the reader is referred to the web version of this article).

Table 2
Modal analysis of studied plutonic rocks.

	Facies	N° of samples	Qz (%)	Kfs (%)	Pl (%)	Bt (%)	Ms (%)	Czo-Ep (%)	Amp (%)	Cpx (%)	Tur (%)	Aln (%)	Grt (%)	Zrn (%)	Spn (%)	Ap (%)	Opq (%)
EL Volcán pluton	EV-l	15	31 ± 3	28 ± 6	31 ± 6	4 ± 3	5 ± 3	0.2 ± 0.5	–	–	<0.1	–	0.5 ± 0.8	<0.1	<0.1	0.4 ± 0.3	0.2 ± 0.3
	EV-g	8	25 ± 4	34 ± 4	22 ± 3	15 ± 3	2 ± 1	0.5 ± 0.8	–	–	–	–	–	<0.1	<0.1	1 ± 0.5	0.4 ± 0.4
	EV-t	2	20 ± 12	–	28 ± 1	20	0.5 ± 0.7	12 ± 2	22 ± 3	–	–	0.1 ± 0.2	–	<0.1	0.9 ± 0.8	0.1 ± 0.1	1.3 ± 1
	EV-md	1	4.5	4.6	30.6	4.2	–	0.5	53	–	–	–	–	<0.1	1.1	1.2	0.3
	EV-s	1	–	27.5	3.4	25.7	–	0.6	24	6.7	–	<0.1	–	–	0.8	0.8	0.5
	Enclav. in EV-g	2	11 ± 4	–	38 ± 1	47 ± 2	0.7 ± 0.3	2 ± 2	–	–	–	–	–	<0.1	<0.1	0.1	<0.1
La Escalerilla pluton	late dykes	6	29 ± 7	30 ± 8	26 ± 6	3.1 ± 3	7.5 ± 7.2	1.1 ± 1.2	–	–	–	–	0.3 ± 0.4	<0.1	0.2 ± 0.3	0.4 ± 0.3	0.2 ± 0.3
	LE-l	14	35 ± 5	33 ± 8	24 ± 9	2.9 ± 2	4.4 ± 2.3	<0.1	–	–	–	<0.1	0.7 ± 0.6	<0.1	0.1 ± 0.2	0.2 ± 0.5	0.4 ± 0.5
	LE-g	15	30 ± 7	32 ± 5	23 ± 5	10 ± 5.3	1.6 ± 1.2	1.6 ± 0.9	–	–	–	<0.1	<0.1	<0.1	0.2 ± 0.3	0.3 ± 0.3	0.2 ± 0.3
	LE-gd	10	33 ± 8	15 ± 5	32 ± 8	13 ± 4	3.2 ± 2	3.4 ± 2.6	–	–	–	0.2 ± 0.2	–	<0.1	<0.1	0.3 ± 0.4	<0.1
	Enclav. in LE- l	1	30	21.4	34	9	3	–	–	–	–	–	0.1	<0.1	–	1.3	1.1
	Enclav. in LE-g	1	11	6	46.3	33	1	1.5	1.2	–	–	–	–	<0.1	–	–	–
	Enclav. in LE-gd	1	12.5	–	18.7	48	–	20	–	–	–	–	–	<0.1	–	–	0.8
#	tonalites	19	24 ± 10	0.5 ± 1	28 ± 9	21 ± 7	0.7 ± 1.2	7.2 ± 5	16 ± 22	–	–	<0.1	<0.1	<0.1	0.1 ± 0.2	0.2 ± 0.2	0.7 ± 0.7
	gabbro-diorites	11	5 ± 2.7	0.1 ± 0.4	30 ± 8	15 ± 10	–	7.6 ± 8.8	42 ± 26	–	–	<0.1	–	<0.1	0.2 ± 0.4	0.2 ± 0.3	1.1 ± 1

The numbers express the percentual mean value ± standard deviation.
(<0.1) = the mineral is present, but was not intercepted by the microscope reticle during the counting.
(#) = representative facies of the Las Verbenas, El Salto, Tinaja (host rock of LEP), Bemberg and Gasparillo plutons.
Abbreviations correspond to Whitney and Evans (2010).

occurs as crystal aggregates, up to 3 mm in size. The grains present deformation bands and subgrains. Plagioclase shows replacement of sericite and clinozoisite-epidote series minerals. K-feldespar is scarce (4–9%) and occurs as interstitial anhedral grains (Fig. 4B). Dark mica is present in limpid crystals with scarce zircon inclusions.

4.1.1.2. Porphyritic biotite-bearing granite facies (LE-g). The LE-g covers the largest area within LEP (approximately 70%), extending from the inflexion zone to the southern part of the Valle de Piedra hill, a short distance (~2 km) northward Potrero de Los Funes locality, in the contact with the EVP (Fig. 2).

It is distinguished by the high dark mica content (10 ± 5.3%) and the presence of K-feldspar phenocrysts (Fig. 4C). According to the modal composition, monzo and syenogranites were identified (Fig. 3). They present porphyritic coarse-grained texture with internal magmatic fabric of NNE direction, outlined by the preferential orientation of the K-feldspar phenocrysts and mica crystals. This orientation is accentuated near the eastern contact, where the fabric is strongly associated with a mylonitic shear zone. Locally ellipsoidal microgranular monzodioritic and tonalitic enclaves (up to 1 m in diameter) are present in this facies. Sporadically, it is also possible to observe xenoliths of metamorphic host-rocks, presumably corresponding to the Micaschists Group (PMC) or San Luis Formation. This facies is made up of quartz, plagioclase (oligoclase-andesine: An_{21-34}), K-feldspar (microcline) and biotite (annite-phlogopite series). The accessory minerals are zircon, epidote-group minerals, sphene, apatite-group minerals (fluorapatite) and opaque (Table 2). Muscovite and epidote-group mineral are also present as secondary phases. Zircon crystals with inherited cores are common (Fig. 4D).

4.1.1.3. Two micas-bearing porphyritic leucogranite facies (LE-l). The LE-1 is present in the northern part of the LEP (Fig. 2). This facies is approximately elongated to the N-S directions, with bottleneck morphology at the north end, given by NE and NW conjugated shear bands (Morosini and Ortiz Suárez, 2010). Locally in the central part, this facies contains large (up to 80 m) roof pendants of tonalitic composition (related to Las Verbenas pluton), and synmagmatic acid dykes are present in the north. Moreover, in the western edge region, the presence of small (~10–90 cm) monzogranitic microgranular enclaves is common. One of the most relevant characteristics is the presence of a greisen-type alteration in the center of the facies and an important local albitization in the western contact with the San Luis Formation.

In contact with the San Luis Formation, north the Las Verbenas tonalitic pluton (Fig. 2), the LEP develops a thermal aureole (300–800 m thick), characterized by a slight increase in the metamorphic grade by temperature rising toward the host rock, given by the occurrence of biotite ± garnet above muscovite + chlorite-group minerals (Morosini and Ortiz Suárez, 2011).

The LE-1 facies is hololeucocratic (CI < 10), the modal composition we identified is monzo and syenogranites (Fig. 3), and its texture is inequigranular porphyritic defined by K-feldspar phenocrysts in a medium-grained matrix (Fig. 4E–F). It essentially consists of quartz, K-feldspar (microcline), plagioclase (albite-oligoclasa: An_{3-14}), biotite (with annite as the dominant component) and muscovite (phengite, primary magmatic); with garnet (spessartite$_{32}$, grossular$_{16}$, pyrope$_2$), apatite-group minerals, zircon and sphene as accessory phases. Secondary minerals such as muscovite, albite and epidote-group minerals locally replace the primary phases (Table 2).

4.1.2. El Volcán pluton (EVP)

The EVP is a plutonic massif with a roughly subcircular morphology, cropping out in the southern sector of the previously called La Escalerilla pluton. It extends from El Volcán in the east up to the reverse neogene faults lifts the Sierra de San Luis in the west, showing a tectonized magmatic contact with the LEP (s.s.) in the north, whereas in the south it is rarely exposed due to the extensive sedimentary cover (Fig. 2). The EVP is composed of several intrusions, predominantly granitic, with subordinated mega enclaves

and dykes of intermediate and mafic compositions. These can be grouped into: 1) a larger body of porphyritic biotite-bearing granite facies (EV-g); 2) dykes and small isolated bodies of a two micas-bearing leucogranite facies (EV-l), 3) mega enclaves of amphibole-bearing monzodioritic and amphibole-bearing tonalitic compositions, and 4) scarce isolated dykes of amphibole and clinopyroxene-bearing syenite (Figs. 2 and 3).

4.1.2.1. Porphyritic biotite-bearing granite facies (EV-g). The EV-g facies covers the largest area of the EVP (Fig. 2). It shows petrographic differences related to LE-g facies (Ordovician) from LEP, which are summarized in: 1) a matrix with a finer texture and lesser sub-solid deformation, 2) higher dark mica content in the matrix, and 3) phenocrysts of K-feldspar more scattered inside the facies (without forming crystal mushes).

The EV-g facies lacks a strong post-magmatic deformation. However, locally sub-solid deformation can be recognized both in the margins and in internal sectors along discrete ductile shears. The EV-g facies and metamorphic host rocks are intruded by swarms of dykes and small bodies assigned to the EV-l facies interpreted as late-magmatic pulses.

In the EV-g facies, the mafic microgranular enclaves of quartz-dioritic composition, up to 50 cm, and locally isolated bodies of sienitic, monzodioritic and tonalitic composition are common (Fig. 2). The EV-g facies consists of rocks with porphyritic texture, made up of K-feldspar phenocrysts in a fine-to-medium grained groundmass. This facies is mainly composed of K-feldspar (microcline), quartz, plagioclase (oligoclasa-andesina: An_{26-44}), biotite (annite-phlogopite series) and muscovite (phengite) in order of abundance. Zircon, epidote-group minerals, apatite and titanite were recognized as accessory minerals. The secondary phases are represented by muscovite and epidote-group minerals. The K-feldspar crystals are up to 8 cm long, locally showing rapakivi texture. In internal ductile shear zones, K-feldspar, biotite and muscovite grains are oriented causing an imperfect foliation. Quartz grains exhibit undulose extinction, deformation lamellae, subgrains, and polygonization tendency. Plagioclase crystals are strongly altered and replaced by muscovite and clinozoisite-epidote series minerals, sporadically showing curved twins and intracrystalline microfractures. Biotite is present as subhedral

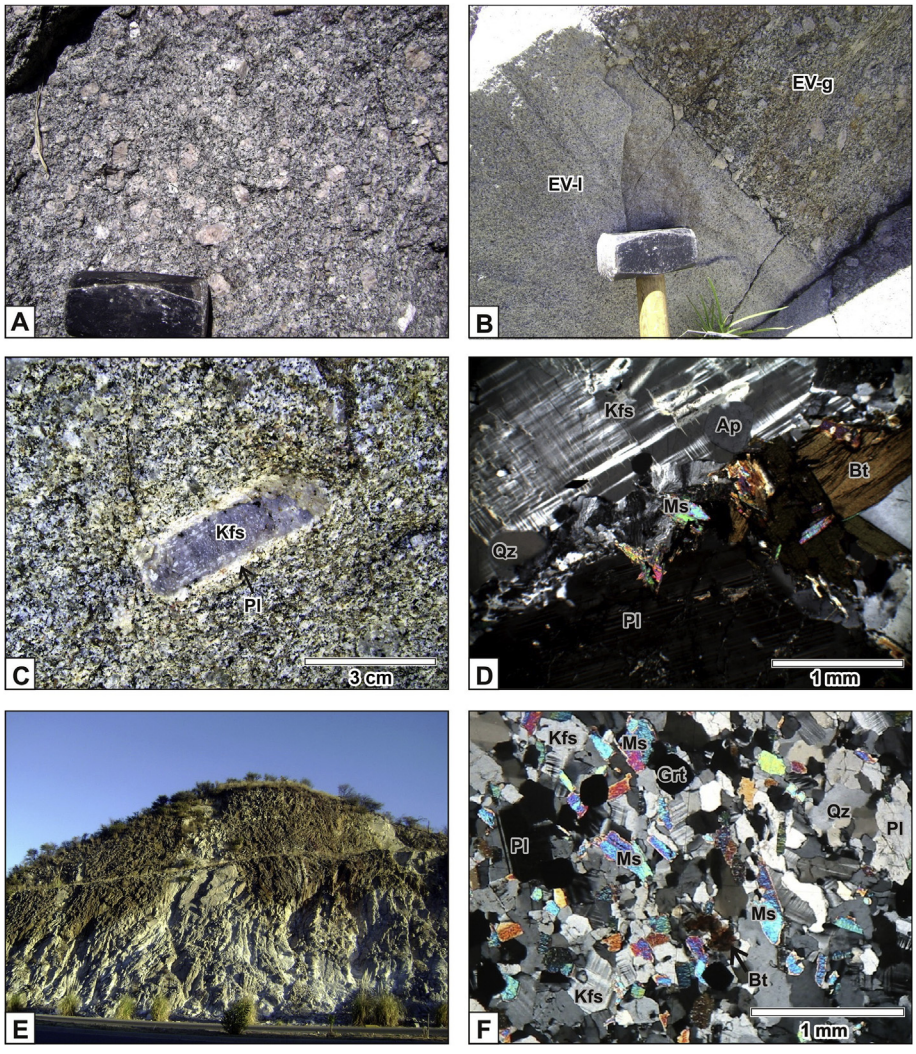

Fig. 5. Photographs corresponding to the outcrop and thin sections of the El Volcán pluton. (A) Texture of the porphyritic biotite-bearing granite facies (EV-g); equidimensional K-feldspar phenocrysts arranged randomly (without deformation). (B) Magmatic contact between equigranular two micas-bearing leucogranite facies (EV-l) and EV-g facies. Some K-feldespar crystals across the contact between both facies are located suggesting that the offset occurred by melt-assisted grain boundary sliding and stopped before final crystallization. (C) Rapakivi feldspar in EV-g facies. (D). Microscopic texture of EV-g facies; myrmekites between K-feldspar and plagioclase crystals are present. (E) Stoping of a small pulse of the EV-l facies in Micaschist Group (east of the El Volcán pluton). Syn-plutonic dykes took advantage of the existing metamorphic foliation planes when magma exerted pressure on the host rock. (F) Photomicrography of EV-l facies; the abundance of muscovite and garnet is common in this rock.

Table 3
LA-MC-ICP-MS U/Pb-zircon data for LE-g facies (sample O22) and EV-g facies (sample AA13).

Sample- Spot	Concentration			Isotopes ratios								Apparent ages (Ma)								
	U (ppm)	Th (ppm)	Th/U	$^{206}Pbc/^{204}Pbm$	$^{206}Pb^*/^{207}Pb^*$	± (%)	$^{207}Pb^*/^{235}U^*$	± (%)	$^{206}Pb^*/^{238}U$	± (%)	Error correction	$^{206}Pb^*/^{238}U^*$	± (Ma)	$^{207}Pb^*/^{235}U$	± (Ma)	$^{206}Pb^*/^{207}Pb^*$	± (Ma)	Best Age (Ma)	± (Ma)	Conc. (%)
Discordant data by loss Pb (deformation)																				
O22-12	1072.6	591.9	0.55	207.97	15.19	21.03	0.58	21.61	0.06	4.95	0.23	398.81	19.14	464.11	80.66	801.64	445.18	398.81	19.14	85.9
O22-4	876.10	515.8	0.59	364.19	15.82	23.51	0.62	23.84	0.07	3.98	0.17	441.99	16.99	489.02	92.78	715.87	505.78	441.99	16.99	90.4
O22-13	647.29	568.5	0.88	471.25	16.19	15.13	0.61	15.41	0.07	2.93	0.19	444.68	12.60	482.37	59.24	665.70	325.70	444.68	12.60	92.2
O22-14	417.31	411.5	0.99	1411.0	17.50	2.98	0.57	11.91	0.07	11.5	0.97	453.57	50.48	460.78	44.13	496.93	65.76	453.57	50.48	98.4
Data used for crystallization age (emplacement)																				
O22-1	757.28	438.4	0.58	647.38	16.70	9.79	0.64	10.12	0.08	2.54	0.25	481.51	11.79	502.60	40.13	599.74	212.49	481.51	11.79	95.8
O22-10	668.95	628.1	0.94	789.13	17.16	4.66	0.61	6.54	0.08	4.59	0.70	468.60	20.72	480.83	25.05	539.56	102.04	468.60	20.72	97.5
O22-11	923.71	820.8	0.89	245.57	15.81	3.14	0.65	3.90	0.07	2.32	0.59	461.81	10.32	507.06	15.56	716.70	66.58	461.81	10.32	91.1
O22-2	777.87	686.8	0.88	1298.5	17.06	4.12	0.65	5.16	0.08	3.11	0.60	496.24	14.88	506.46	20.59	552.89	89.87	496.24	14.88	98.0
O22-3	457.93	155.4	0.34	1158.8	16.75	8.94	0.64	9.13	0.08	1.85	0.20	480.64	8.55	500.59	36.11	592.85	194.24	480.64	8.55	96.0
O22-7	650.76	296.5	0.46	1349.2	17.33	4.94	0.63	5.44	0.08	2.29	0.42	489.74	10.82	494.73	21.32	517.91	108.42	489.74	10.82	99.0
O22-8	996.18	402.7	0.40	312.50	16.05	11.04	0.64	11.25	0.07	2.17	0.19	465.42	9.75	504.22	44.74	684.38	236.32	465.42	9.75	92.3
O22-9	932.02	1259	1.35	192.65	14.95	5.62	0.70	7.27	0.08	4.61	0.63	472.38	20.98	539.53	30.44	834.44	117.29	472.38	20.98	87.6
Age data of an inherited core (source)																				
O22-6	454.22	315.7	0.69	14,108	16.97	2.77	0.72	4.04	0.09	2.95	0.73	545.62	15.43	549.28	17.15	564.48	60.24	545.62	15.43	99.3
O22-5	539.27	384.6	0.71	4417	17.40	2.71	0.72	3.78	0.09	2.64	0.70	557.41	14.08	548.00	16.03	509.03	59.70	557.41	14.08	101.7
Discordant data by loss Pb (deformation)																				
AA13-6	625	794.8	1.27	480	16.25	19.8	0.481	20.0	0.056	3.0	0.15	356.2	10.3	399.2	66.0	657.0	427.5	356.2	10.3	89.2
AA13-7	714	1032.8	1.45	487	17.24	10.4	0.469	11.1	0.058	3.9	0.35	367.4	13.8	390.5	36.1	529.5	229.5	367.4	13.8	94.1
AA13-9	676	407.3	0.60	1353	17.68	3.0	0.463	4.5	0.059	3.3	0.74	372.2	12.0	386.6	14.4	473.6	66.2	372.2	12.0	96.3
Data used for crystallization age (emplacement)																				
AA13-1	374	305.9	0.82	4358	18.19	2.0	0.504	6.4	0.066	6.1	0.95	415.6	24.7	414.9	21.9	411.1	43.7	415.6	24.7	100.2
AA13-12	450	82.3	0.18	2783	17.88	2.8	0.504	6.7	0.065	6.1	0.91	408.4	24.3	414.5	22.9	448.6	61.2	408.4	24.3	98.5
AA13-13	447	114.5	0.26	756	17.07	7.0	0.514	9.7	0.063	6.7	0.69	398.5	25.8	421.8	33.5	551.0	153.8	398.5	25.8	94.5
AA13-2	469	599.2	1.28	6941	17.26	3.7	0.522	4.3	0.065	2.2	0.51	408.4	8.6	426.7	14.9	526.4	80.6	408.4	8.6	95.7
AA13-3	269	343.6	1.28	21,019	18.03	3.5	0.501	4.4	0.065	2.6	0.59	409.7	10.2	412.8	14.9	430.5	79.1	409.7	10.2	99.2
AA13-4	438	712.8	1.63	3448	17.60	4.5	0.500	5.3	0.063	2.8	0.53	399.0	10.9	411.8	17.9	484.0	98.7	399.0	10.9	96.9
AA13-5	512	437.6	0.85	3733	15.62	13.5	0.565	13.6	0.064	1.9	0.14	400.6	7.2	455.2	50.0	741.4	286.7	400.6	7.2	88.0

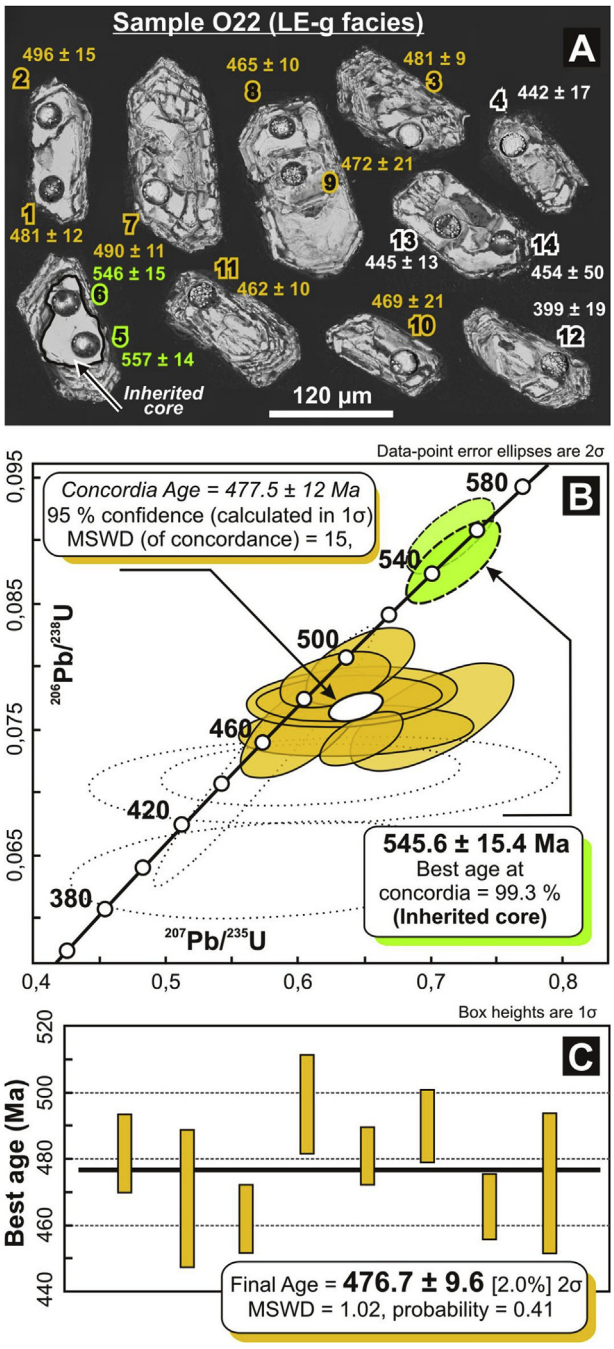

Fig. 6. Ages of zircons in sample O22 belonging to the LE-g facies (La Escalerilla pluton). (A) Backscattered electron image of the analyzed zircons, generated ablation pits during the analysis are observed. (B) Conventional concordia diagram. Errors are shown as ellipses at the 2σ level. Three groups of ellipses are shown, the major one corresponding to Ordovician crystallization (solid-line yellow ellipses), with a concordia age calculated for this group, another group belongs to ages from an inherited core (dashed-line green ellipses), and one representing discordant ages for Pb loss (transparent dotted-line ellipses) that have not been weighted when the final age was determined. (C) Final Age, calculated by averaging the $^{206}Pb/^{238}U$ apparent ages with highest concordance. The results were plotted with *Isoplot/Excel* (Ludwig, 2003). (For interpretation of the references to colour in this figure legend, the reader is referred to the web version of this article.)

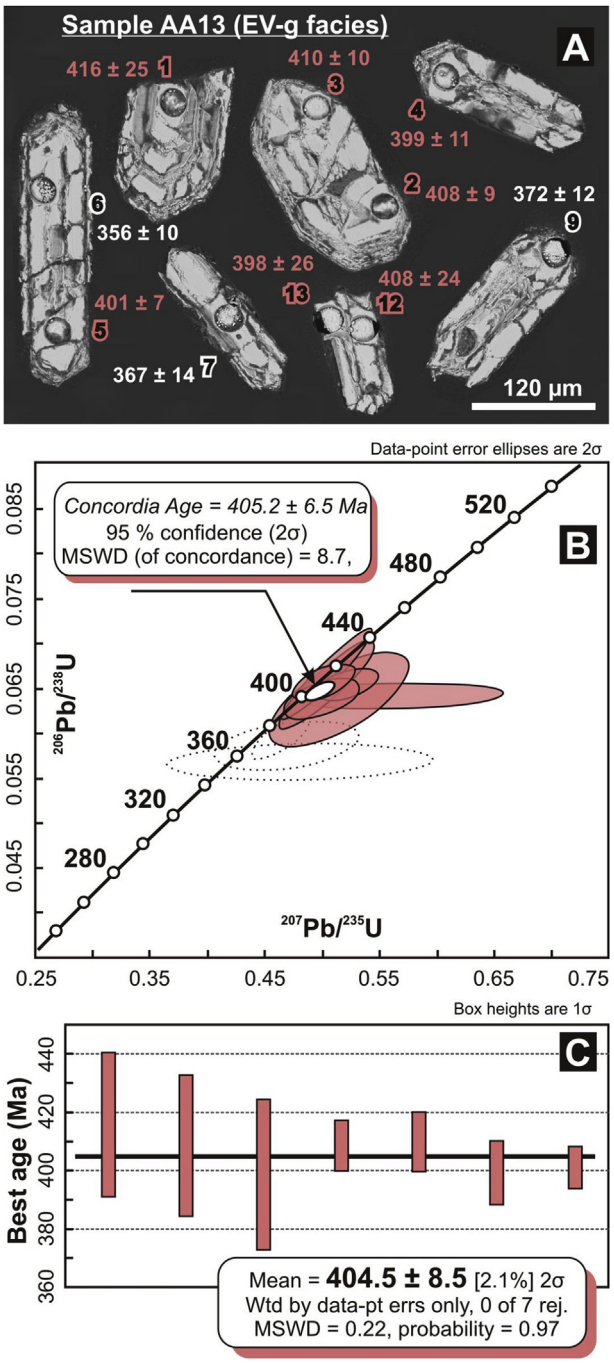

Fig. 7. Ages of zircons in the sample AA13 belonging to the EV-g facies (El Volcán pluton). (A) Backscattered electron image of the analyzed zircons. (B) Conventional concordia diagram. Errors are shown as ellipses at the 2σ level. Two groups of ellipses are shown, the major one corresponding to Devonian crystallization (pink ellipses of solid line) with a concordia age calculated for this group, another group representing discordant ages for Pb loss (dotted line ellipses) that have not been weighted when the final age was determined. (C) Final Age, calculated by averaging the $^{206}Pb/^{238}U$ apparent ages with the highest concordance. The results were plotted with *Isoplot/Excel* (Ludwig, 2003). (For interpretation of the references to colour in this figure legend, the reader is referred to the web version of this article.)

grains including pristine crystals of zircon (up to 0.03 cm) and titanite.

4.1.2.2. Two micas-bearing leucogranite facies (EV-l). The EV-l facies is widely distributed in the eastern sector of EVP (Fig. 2). It occurs mostly as dykes and small bodies (Fig. 5E) surrounded into the plutonic EV-g facies and into the metamorphic host rocks, representing the final magmatic differentiates of EVP. The dykes present variable thicknesses ranging from 10 cm to several meters. Within

Table 4
Whole-rock chemical analyses for dated granitic facies.

Pluton	La Escalerilla			El Volcán		
Facies	Biotite porphyry granite (LE-g)			Biotite porphyry granite (EV-g)		
Sample	237D	Z24	316	1-EVG	333A	125
Major elements (wt. %)						
SiO_2	65.32	70.21	61.26	60.65	65.02	59.43
Al_2O_3	14.25	13.19	14.87	15.58	14.41	18.22
Fe_2O_3t	6.68	4.12	7.72	6.85	4.68	4.68
MnO	0.174	0.109	0.148	0.107	0.087	0.086
MgO	1.9	1.1	2.45	2.44	1.66	1.8
CaO	2.2	1.84	3.47	3.1	2.31	3.12
Na_2O	2.44	2.57	2.25	3.3	3.09	3.99
K_2O	4.48	4.56	5.13	4.17	4.17	5.22
TiO_2	0.963	0.553	1.151	1.276	0.765	1.012
P_2O_5	0.38	0.19	0.44	0.72	0.49	0.51
LOI	1.07	0.88	1.33	2.06	1.81	1.57
Total	99.8	99.3	100.2	100.3	98.5	99.64
Trace elements (ppm)						
Sc	22	12	24	10	9	10
Be	3	3	3	4	5	7
V	110	62	137	107	74	86
Cr	<20	<20	<20	20	<20	<20
Co	11	7	14	11	8	9
Ni	<20	<20	<20	<20	<20	<20
Cu	10	<10	10	<10	<10	<10
Zn	110	80	110	110	120	70
Ga	21	18	20	28	26	25
Ge	1.8	1.9	1.7	1.6	1.3	1.2
As	<5	<5	<5	<5	<5	<5
Rb	331	373	272	261	243	197
Sr	98	73	125	664	603	1192
Y	60.5	66	51.8	52.4	27.4	30.5
Zr	480	298	529	573	358	409
Nb	29	26.7	21.7	38.7	22.7	22.1
Mo	<2	<2	<2	<2	<2	<2
Ag	<0.5	<0.5	<0.5	<0.5	<0.5	<0.5
In	0.1	<0.1	<0.1	<0.1	<0.1	<0.1
Sn	9	10	5	9	6	7
Sb	3.7	5	3.2	<0.2	3.5	2.6
Cs	16.3	38.2	18.8	19.8	17.7	5.4
Ba	445	300	544	1072	1182	1720
La	124	62.1	93.5	177	128	211
Ce	259	132	189	309	235	340
Pr	27.1	13.8	19.4	37.1	24.1	36.5
Nd	95.3	49.4	67.1	132	64.9	98.2
Sm	20	10.8	12.8	19.1	11.3	15
Eu	1.95	1.14	1.83	4.06	2.4	3.61
Gd	15.9	9.77	10.8	12.1	7.29	8.63
Tb	2.19	1.69	1.57	1.71	0.91	0.96
Dy	11.7	10.3	8.84	8.94	4.72	4.87
Ho	2.16	2.12	1.77	1.73	0.89	1
Er	5.94	6.51	5.23	5.33	2.53	3.02
Tm	0.792	1.01	0.755	0.856	0.363	0.446
Yb	4.6	6.62	4.65	6.05	2.29	2.92
Lu	0.655	0.961	0.697	0.931	0.346	0.435
Hf	10.7	7.4	11.3	14.8	7.6	8.6
Ta	1.9	4.27	1.09	5.43	2.24	2.88
W	0.7	1.6	1.3	0.7	1.1	<0.5
Tl	2.75	3.21	2.23	1.87	1.89	0.82
Pb	24	37	18	34	37	18
Bi	0.3	0.5	1	1.5	0.2	0.2
Th	81.6	53.5	35.4	75.5	31.7	44
U	3.26	4.48	5.83	6.22	6.05	4.98
Sr/Y	1.62	1.11	2.41	12.67	22.01	39.08

the EVP they have directions of WNW-ESE to NW-SE with dips predominantly toward NE. In the metamorphic rocks, dykes are emplaced with preferential N-S strikes, following the foliation of the host-rock, although in some sectors they are locally cut accross transversely to the foliation. They have flow fabric given by the accumulation of minerals (Bt, Ms and Grt) in parallel bands (Fig. 5B). EV-l facies can be classified as leuco-monzogranites (Fig. 3) with color index <10. This is a heterogeneous rock, normally of medium-grained texture, but locally varying from pegmatitic in the core to aplitic in the borders of the dykes. The rocks with pegmatitic texture are better exposed in the shear zone along the contact between EVP and the Micaschist Group (Fig. 2) where they are strongly milonitized.

The EV-l facies (dykes and major bodies) is primarily composed of quartz, plagioclase (oligoclase: An_{15-18}), muscovite (phengite), biotite (annite-phlogopite series) and K-feldespar (microcline), and, as accessories, tourmaline (schorl), garnet-group minerals, apatite-group minerals and zircon (Table 2 and Fig. 5F). Quartz occurs as polycrystalline xenomorphic aggregates, from 1 mm in aplites to 3 mm average in zones with coarser texture. K-feldspar is present in anhedral crystals and xenomorphic polycrystalline aggregates. Plagioclase is somewhat larger than other minerals and is mostly altered to sericite. Muscovite forms subhedral grains from 0.2 to 3 mm and biotite is scarce and appears as subhedral individuals, normally with zircon inclusions. Tourmaline was not detected in thin sections, but was recognized in outcrops.

4.2. Zircon U-Pb dating of the studied plutons

Data of isotopic ratios and the estimation of apparent isotopic ages for studied granites of La Escalerilla and El Volcán plutons, respectively, are presented in Table 3.

The analyzed zircon crystals of LE-g facies (sample O22) are generally euhedral to subhedral (magmatic), their size ranging from 120 to 250 μm in length, showing a typical internal zoning, and some crystals exhibit cores with discordant contours with respect to the zoning of crystal magmatic growth, indicating that these are inherited cores (Fig. 6A). But it is important to point out that the carrier rock of these zircons presents subsolidus deformation, which is the reason why we believe that some analyses of zircons show significant loss of Pb, and these analyses have not been subjected to the calculation of crystallization final age.

The final age of crystallization determined for the LE-g facies in the inflexion zone (sample O22) is typically Famatinian: 476.7 ± 9.6 Ma, being the concordia age of 477.5 ± 12 Ma (95% confidence) using a group of eight best concordance data between $^{206}Pb/^{238}U$ and $^{207}Pb/^{235}U$ apparent ages. Ages of 557.4 ± 14 Ma and 545.6 ± 15.4 Ma correspond to an inherited zircon core, the latter being the age that best fits the concordia (Fig. 6B–C).

Furthermore, in the EV-g facies (sample AA13 of El Volcán pluton), magmatic zircons yield a final age of 404.5 ± 8.5 Ma, with a concordia age of 405.2 ± 6.5 Ma (95% confidence) using the best seven concordance data-point (Fig. 7). The zircons of this granite are pristine and do not present inherited cores (although the data from statistical analyses do not allow us to confirm this assertion). However, in some analyses low Pb values are observed, presumably because this granite also has a degree of sub-solid deformation.

The results of the samples analyzed have a high degree of reliability, with a value of MSWD = 1.02 for sample O22 from the inflexion zone of the La Escalerilla pluton and a moderate probability of 0.41%. In turn, a value of MSWD = 0.22 for sample AA13 from the El Volcán pluton represents a much lower scatter of the used data points than expected by analytical errors, with a very good probability value of 0.97%.

4.3. Whole rock geochemistry of the dated granites

The major and trace element compositions of selected samples of the granitic facies from LEP and EVP are quoted in Table 4. The rocks have similar concentrations of major elements but different REE and trace element contents (Table 4 and Figs. 8 and 9). They are slightly to moderately peraluminous, although one sample (316)

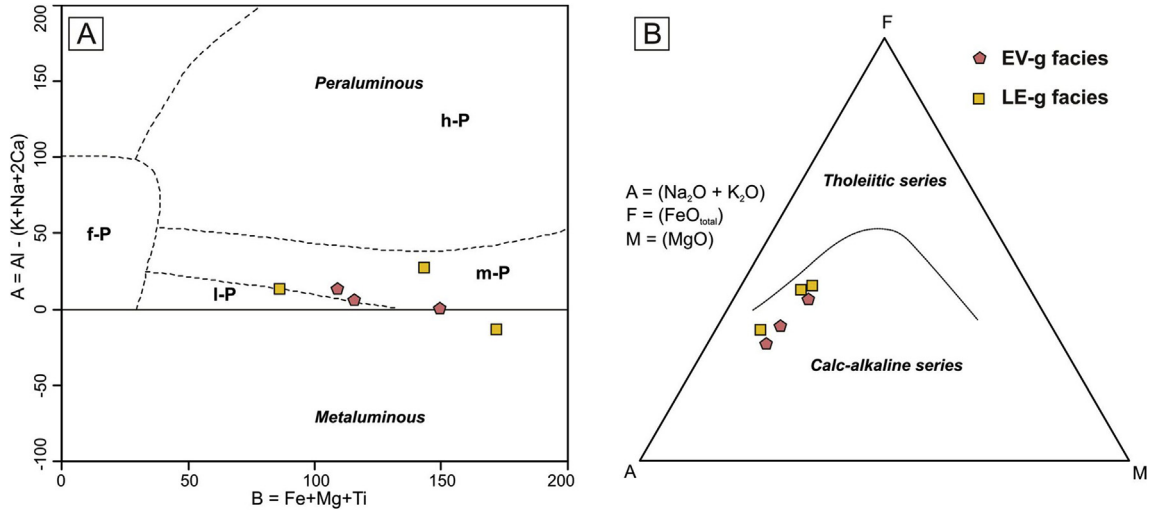

Fig. 8. Major elements diagrams. (A) Villaseca et al. (1998); both granites are from lowly peraluminous (l-P) to moderately peraluminous (m-P), but one sample is metaluminous near the m-P limit. (B) Irvine and Baragar (1971); the granites are located very close to each other within the AFM diagram, both are part of the calc-alkaline series, and moderately evolutioned.

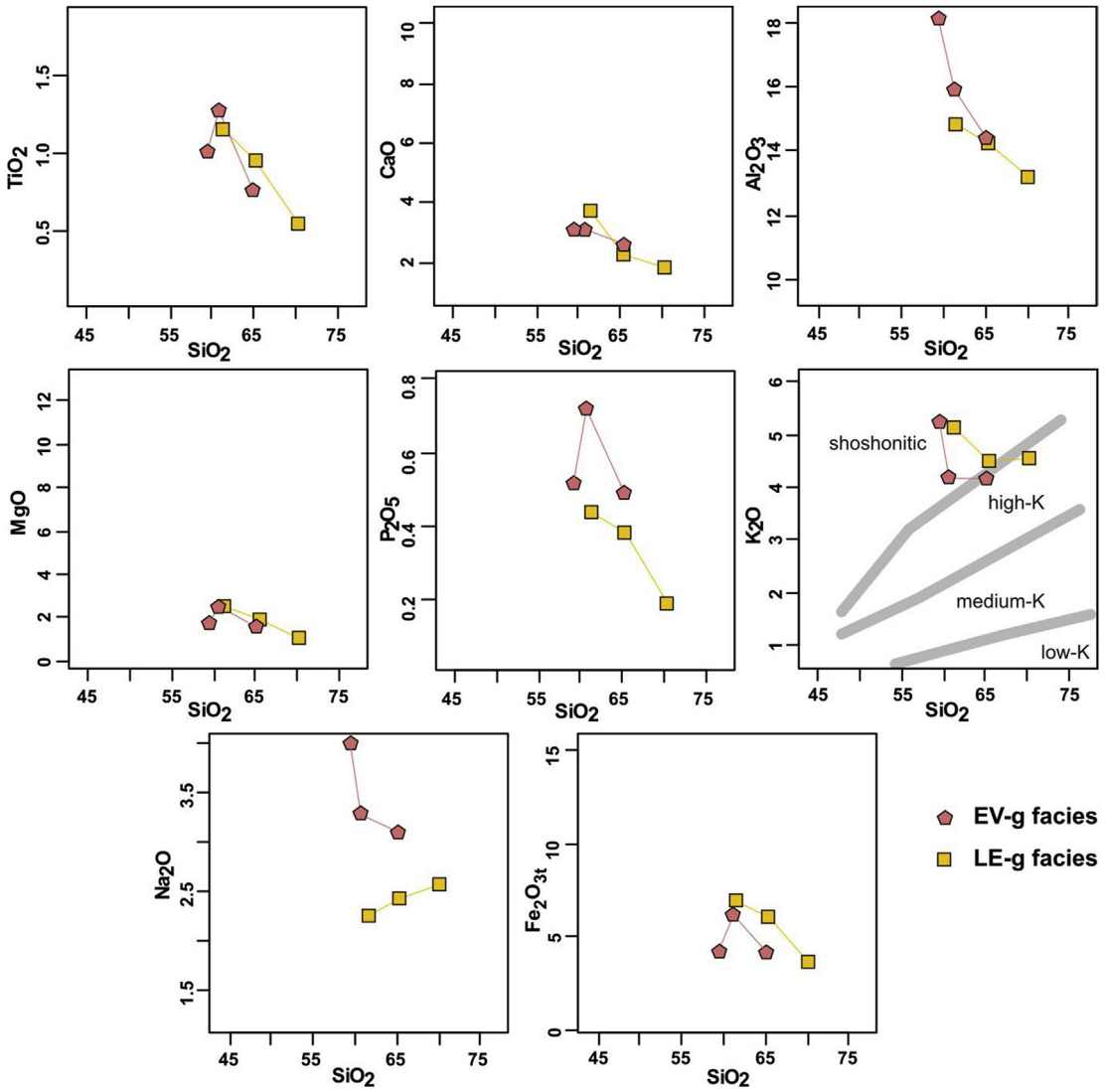

Fig. 9. Harker diagrams. Similar concentrations of major elements with respect to differentiation grade are observed, except Na_2O, P_2O_5 and Al_2O_3, which are slightly higher for the EV-g facies. The K_2O vs SiO_2 diagram shows the proposed fields by Peccerillo and Taylor (1976).

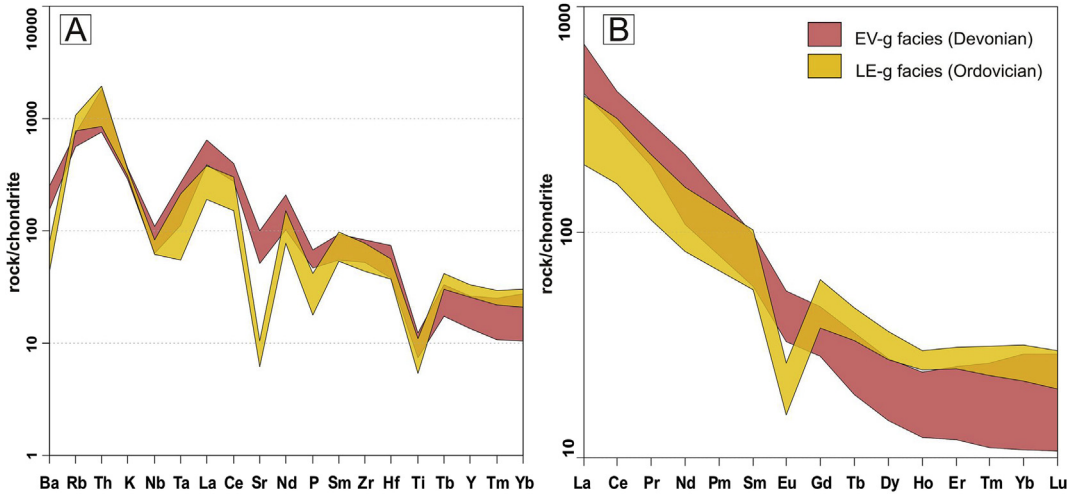

Fig. 10. Trace elements diagrams for the dated granitic facies. (A) Chondrite-normalized multi-element diagram (Thompson, 1982). (B) Chondrite-normalized REE diagram (Boynton, 1984).

plot in the metaluminous field near the m-P limit (Fig. 8A). In the AFM diagram (Irvine and Baragar, 1971) they plot in a restricted field within the calc-alkaline series (Fig. 8B). The LEP and EVP are high-K to shoshonitic granites with normal and very similar trends (except to Na_2O, Al_2O_3 and P_2O_5), as is indicated by the Harker variation diagrams (Fig. 9).

The trace elements pattern normalized to chondrite values shows a general LILE enrichment and HFSE depletion. The *spider* diagram (Fig. 10A) shows that the granitic facies of the EVP, in relation to those of the LEP are comparatively richer in Ba, Sr, Nb, La,

Table 5
compilation of ages reported so far in the study area

Units	Ages (Ma)	Dating method	Authors
Ages of late to postorogenic crystallization			
El Volcán pluton (*EV-g facies*)	405 ± 9	LA-MC-ICP-MS U/Pb-zircon	Morosini et al. **(this work)**
La Escalerilla pluton *(now "El Volcán")*	397 ± 10	K/Ar-biotite	López de Luchi et al. (2002)
La Escalerilla pluton *(now "El Volcán")*	403 ± 6	SHRIMP U/Pb-zircon	Sims et al. (1998)
El Molle Granite	417 ± 7	Convencional U/Pb-zircon	Sato et al. (2003b)
El Molle Granite	380 ± 7	K/Ar-biotite	Steenken et al. (2008)
Ages of orogenic crystallization			
La Escalerilla pluton (*LE-g facies*)	477 ± 10	LA-MC-ICP-MS U/Pb-zircon	Morosini et al. **(this work)**
La Escalerilla pluton (*LE-l facies*)	507 ± 24	Convencional U/Pb-zircon	von Gosen et al. (2002)
Pantanos Negros Granite	477 ± 5	Convencional U/Pb-zircon	Sato et al. (2003b)
Río Claro Granite	490 ± 15	Convencional U/Pb-zircon	von Gosen et al. (2002)
La Verbenas Tonalite	478 ± 4	SHRIMP U/Pb-zircon	Steenken et al. (2006)
Gasparillo Tonalite	~472	Convencional U/Pb-zircon	Sato et al. (2004)
Bemberg Tonalite	468 ± 6	SHRIMP U/Pb-zircon	Sims et al. (1998)
Ages interpreted in accordance with the climax of the main famatinian regional metamorphism (M2)			
NMC (leucocratic monzogranite)	460 ± 12	PbSL-garnet	Steenken et al. (2006)
NMC (migmatite)	478 ± 4	U/Pb-monazite	Steenken et al. (2006)
NMC (orthogneiss)	473 ± 3	U/Pb-monazite	Sato et al. (2005)
NMC (orthogneiss)	475 ± 3	U/Pb-monazite	Sato et al. (2005)
NMC (Sil-Grt gneiss)	458 ± 3	Convencional U/Pb-zircon	González et al. (2002)
NMC (Sil-Grt gneiss)	470 ± 15	Chem. dating (monazite)	González et al. (2002)
NMC (Sil-Grt gneiss)	445 ± 21	Sm/Nd (W.R. and M)	González et al. (2002)
NMC (amphibolite)	476–457	Ar/Ar-amphibole	González et al. (2002)
NMC (amphibolite)	452 ± 23	K/Ar-amphibole	Ortiz Suárez (1999)
PMC (Sil-Grt gneiss)	460–450	SHRIMP U/Pb-zircon	Sims et al. (1998)
PMC (granulite)	498 ± 10	SHRIMP U/Pb-zircon	Steenken et al. (2006)
PMC (Grt gneiss)	452 ± 19	PbSL-garnet	Steenken et al. (2006)
PMC (Grt gneiss)	454 ± 18	K/Ar-amphibole	Steenken et al. (2006)
PMC (amphibolite)	466 ± 23	K/Ar-amphibole	Ortiz Suárez (1999)
PMC (orthogneiss)	484 ± 7	SHRIMP U/Pb-zircon	Sims et al. (1997)
PMC - (Las Águilas ultramafic rocks)	478 ± 6	SHRIMP U/Pb-zircon	Sims et al. (1997)
Cooling ages interpreted in accordance with the closure of the last famatinian metamorphic event (M3)			
La Escalerilla pluton (*mylonitic granite?*)	360 ± 8	K/Ar-muscovite	Steenken et al. (2008)
La Escalerilla pluton (*mylonitic granite?*)	414 ± 14	Errochr. Rb/Sr (W.R.)	Llambías et al. (1998)
La Escalerilla pluton (*mylonitic granite*)	366 ± 2	K/Ar-muscovite	Sims et al. (1998)
Bemberg Tonalite *(recrystallised phases?)*	361 ± 8	K/Ar-biotite	Steenken et al. (2008)
La Verbenas Tonalite *(recrystal. phases?)*	371 ± 8	K/Ar-biotite	Steenken et al. (2008)
NMC *(shear zone)*	414–364	K/Ar-biotite	Sato et al. (2001)
PMC *(La Arenilla shear zone – central)*	366 ± 2	Ar/Ar-muscovite	Sims et al. (1998)
PMC *(La Arenilla shear zone – southern)*	375 ± 1	Ar/Ar-muscovite	Sims et al. (1998)

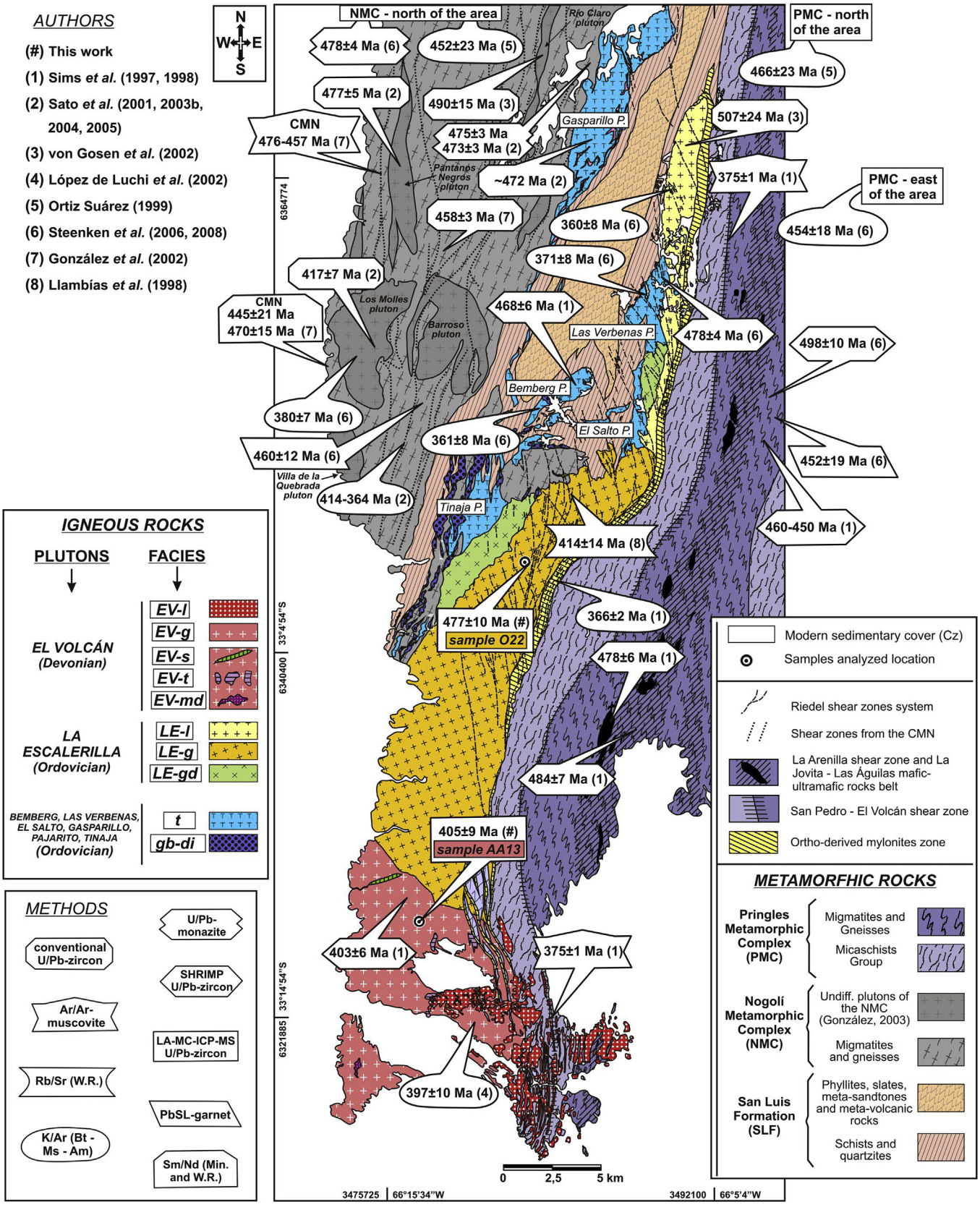

Fig. 11. Map of ages determined in this work and by other authors in the study area. Ordovician ages of magmatic crystallization linked to main Famatinian regional metamorphism (M2) are showed, as well as Devonian ages associated with cooling of shear zones (M3) which resulted in the exhumation of Nogolí and Pringles Complexes during the collisional stage in Silurian period.

Ce, P, and poorer in Rb, Tb, Y, Tm and Yb. The EVP rocks are notably enriched in Sr and depleted in Y, resulting in high Sr/Y ratios (12.67–39.08) compared to LEP (1.11–2.41) (Table 4).

Chondrite-normalized REE values show that both granites are significantly enriched in LREE and depleted in HREE. However, two different pattern designs are apparent from Fig. 10B. The LEP granitic rocks have La/Yb_N with a range of 6.3–18.1, and negative Eu anomalies ($Eu/Eu^* = 0.33$ to 0.48); while the EVP granitic facies show higher La/Yb_N ratios (9.0–37.6) and insignificant negative Eu anomalies ($Eu/Eu^* = 0.8$).

5. Discussion and interpretation

5.1. Geochronology significance

The LEP (s.l.) has been previously considered to be only one granitic body of the pre-deformational Famatinian orogeny (Ortiz Suárez et al., 1992; Sato et al., 1996; Llambías et al., 1998; von Gosen et al., 2002; Brogioni et al., 2005), as well as of the Achalian orogeny (Sims et al., 1998; López de Luchi et al., 2002; 2007; Steenken et al., 2006, 2008), based on field relationships and isotopic ages, respectively. However, von Gosen et al. (2002) determined an age of 507 ± 24 Ma (conventional U/Pb-zircon) for the northern portion of the body, and proposed a Devonian pluton in the southern sector, according to the age obtained by Sims et al. (1998), and which the authors called El Volcán.

Based on new U-Pb ages, whole rock chemical data and detailed field relationships, we support the existence of the EVP. The U-Pb ages (403 ± 6 Ma, SHRIMP U/Pb-zircon) obtained by Sims et al. (1998) in the southern sector of the La Escalerilla pluton (s.l.) correlated well with the age of 404.5 ± 8.5 Ma (LA-MC-ICP-MS U/Pb-zircon) obtained in this work from granitic rocks in the same area.

The new age of 476.7 ± 9.6 Ma (LA-MC-ICP-MS U/Pb-zircon) obtained in this work from granitic rocks cropping out in the infection zone (La Escalerilla homocline) restricts the possibility for considering that all rocks that compose the La Escalerilla pluton (s.l.) correspond to a Devonian age, as proposed by Sims et al. (1998), Stuart-Smith et al. (1999), Steenken et al. (2006) and López de Luchi et al., 2007. Taking into account published and new data, the LEP (s.l.) should be divided into two plutons, LEP (s.s.) in the north, and EVP in the south.

Furthermore, the crystallization age obtained in this work for the LE-g facies (inflexion zone) is very similar to the Ordovician ages obtained by other authors in the tonalitic and granitic bodies present in the near environment (Sims et al., 1998; von Gosen et al., 2002; Sato et al., 2003b, 2004; Steenken et al., 2006), which are summarized in Table 5 and Fig. 11. Therefore, the early synkinematic Ordovician age of LEP would be confirmed with respect to the main phase of the Famatinian orogeny, which is assumed to be within an interval of ~478 to ~450 Ma (Sato et al., 2003a). It should be pointed out that the age of 507 ± 24 Ma (conventional U/Pb-zircon) determined by von Gosen et al. (2002) in the northern sector of La Escalerilla pluton (LE-l facies) does not match the scheme proposed in the present study. We consider that this age is not consistent with the field relationships, because the LE-l facies is more differentiated and, consequently, more recent than the LE-g facies, here dated at 477 ± 10 Ma. Moreover, the intrusive contact (with stoping) that presents the LE-l facies over the Las Verbenas tonalitic body (Sato and Llambías, 1994; Morosini, 2011), whose age was calculated at 478 ± 4 Ma (SHRIMP U/Pb-zircon, Steenken et al., 2006), restricts the age of LE-l facies.

In general terms, the existing absolute ages show a marked contemporaneity between the LEP and the tonalitic plutons, and for

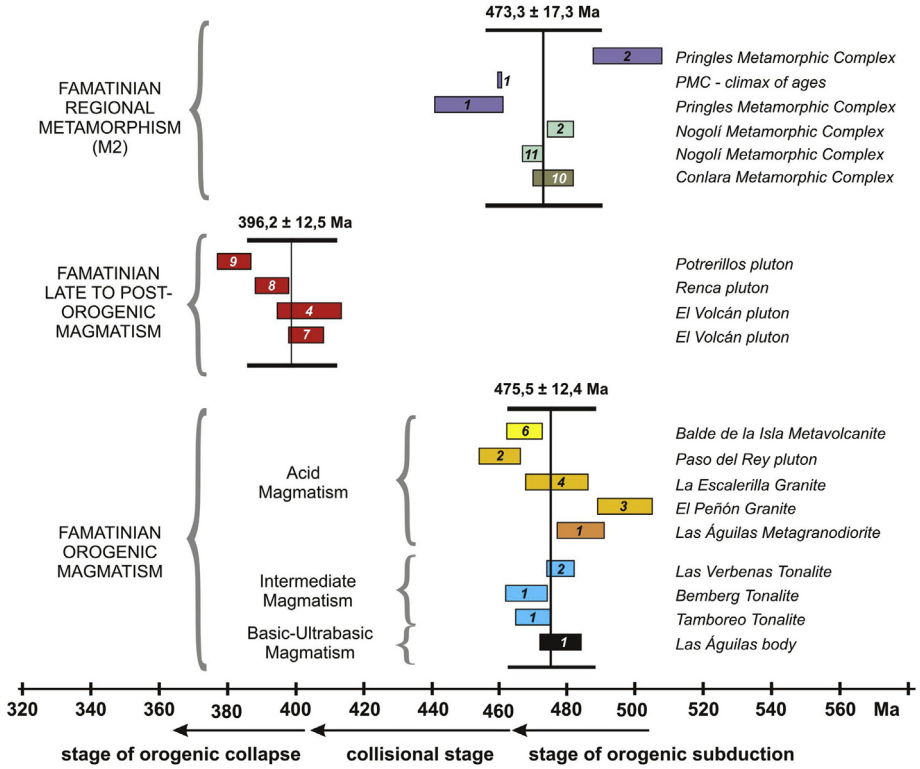

Fig. 12. Scheme of evolution for the Famatinian magmatism of the Sierra de San Luis considering the most reliable ages (SHRIMP and LA-MC-ICP-MS U/Pb-zircon or U/Pb-monazite). The average ages and the range of uncertainty calculated for each group (main metamorphism, orogenic and post-orogenic magmatism) are shown. (1) Sims et al. (1998); (2) Steenken et al. (2006); (3) Steenken et al. (2005); (4) This work; (5) Sato et al. (2003a); (6) Casquet et al. (2014); (7) Sims et al. (1997); (8) Stuart-Smith et al. (1999); (9) Siegesmund et al. (2004); (10) Whitmeyer and Simpson (2004); (11) Carugno Durán and Ortiz Suárez (2012).

that reason, we decided to group all the Ordovician plutons of the area investigated in the so-called "Valle de Pancanta Plutonic Complex" (VPPC) (Fig. 2).

Contemporaneity between I- and S-type granitoids in only one tectonic environment of Ordovician age was recognized by Sato et al. (2003a), Brogioni et al. (2005) and López de Luchi et al. (2007) in the Sierra de San Luis, and by Pankhurst et al. (2000) and others in several localities of the Famatinian belt, during a time period which spans from 499 to 468 Ma.

The ages presented in Table 5 and Fig. 11 show that there is an overlap between the orogenic magmatism (Ordovician) and metamorphism linked to Famatinian climax (M2), as well as between Devonian plutonic intrusions and latest stages of the metamorphic episode M3, indicating the orogenic collapse. In addition, a strong body of evidence of contemporaneity between metamorphism and basic, intermediate and acid magmatism for the Famatinian orogeny is reflected in the absolute ages of greater confidence (SHRIMP and LA-MC-ICP-MS U/Pb-zircon or U/Pb-monazite methods) determined by different researchers in the Sierra de San Luis (Fig. 12).

5.2. Geochemical significance

Chondrite-normalized REE patterns of the LE-g facies display a gull-wing shape (Fig. 10B), indicating, together with low Sr/Y values, that plagioclase was a stable phase that fractionated Sr and Eu^{2+} at source. In contrast, the high degree of LREE fractionation with respect to HREE, the absence of Eu anomaly and the high Sr/Y values suggest that magmatic differentiation for EV-g facies occurs outside the stability field of plagioclase and within that of amphibole ± garnet, because Y strongly partitioned into both amphibole and garnet during partial melting or magmatic fractionation processes (Chiaradia, 2015). These assumptions about the geochemical results show that the studied granites have different origins. Sr/Y is a common qualitative indicator of the average crustal pressure, or depth, at which magmatic differentiation occurred (Paterson and Ducea, 2015). A larger Sr/Y ratio signifies a greater pressure or depth (Chapman et al., 2015). Low Sr/Y values (<10), for magmas with concentrations less than 3 wt% MgO, are stadistically more common of arcs <20 km thick, where the magmatic differentiation occurs in the stability field of plagioclase, the main host of Sr in magmatic rocks especially during early differentiation processes. In contrast, high Sr/Y values (15–35), for magmas with concentrations less than 3 wt% MgO, are stadistically common of arcs >30 km thick, where magmatic differentiation occurs outside the stability field of plagioclase and within that of amphibole ± garnet (Chiaradia, 2015).

Therefore, we can infer that the LE-g facies (Sr/Y = 1.11 to 2.41) would have separated from its source at depths no greater than 25 km (<~0.7 GPa), because plagioclase starts to be very unstable from those depths onwards (e.g. Patiño Douce and Beard, 1995). In contrast, the EV-g facies (Sr/Y = 12.67 and 39.08) would have been separated from its source at depths greater than 30 km (>~0.8 GPa), in the amphibole ± garnet stability field.

These interpretations allow to deduce there was a thin crust at the time that the LE-g facies (La Escalerilla pluton) was fractioned from its source, indicating that melting took place in a stage of pre-collisional arc of subduction, probably linked to a back-arc sub-environment (Brogioni, 1994; Larrovere et al., 2011). On the contrary, previous interpretations suggest there was a thick crust at the time melting occurred which gave origin to the EV-g facies (El Volcán pluton), and this is consistent with the ages obtained that indicate an emplacement after a tectonic exhumation with cortical thickening due the collision stage. In this regard, there is a great similarity between the concentrations of majority and trace elements in the EV-g facies (El Volcán pluton) with respect to other post-orogenic plutons of the Sierra de San Luis, such as Renca, La Totora, El Hornito and Las Chacras-Potrerillos, according with López de Luchi et al. (2007). These authors believe that all Devonian granitoids are defined by a melting trend between 0.7 and 1.0 GPa and that the lamprophyres associated with this magmatism indicate low-grade of melting of metasomatized lithospheric mantle, this signal of mantle in the El Volcán pluton would be represented by amphibole-bearing monzodioritic mega-enclaves and dykes of amphibole and clinopyroxene-bearing syenites.

6. Conclusions

The results obtained in this work show that there are distinctive geochemical characteristics and different absolute ages for the granitic rocks studied and show that what had been considered to be a single granite pluton [La Escalerilla (s.l.)] corresponds to two composites plutons: La Escalerilla [s.s. (477 ± 10 Ma)], and El Volcán (405 ± 9 Ma). Particularly the concentrations of trace elements (e.g. Sr/Y ratios) in granitic facies of both plutons indicate that the separation from their sources in the two magmatic groups occurred at different depths; below 25 km for the LEP and above 30 km for the EVP, indicating distinctive geotectonic environments; in the first case (LEP), a thin crust linked to an environment of pre-collisional subduction, while in the second case (EVP), a thickened crust of post-collisional environment whose magmatism marks the beginning of the orogenic collapse.

An important point to consider is that the sequence of geological events, based on the absolute ages (determined by us and other authors) and field relationship between the different facies that make up the La Escalerilla pluton and tonalitic bodies of the area (Gasparillo, Las Verbenas, El Salto, Bemberg and Tinaja plutons), demonstrates a common geotectonic history, and for this reason we define the "Valle de Pancanta Plutonic Complex" (VPPC), dated between 480 and 468 Ma (Lower to Middle Ordovician). In addition, the field relationship between the VPPC and the metamorphic host rocks shows that the orogenic history in the study area can be clearly explained into the Ordovician-Silurian period, with the development of a subduction arc between ~490 and ~465 Ma (intrusion of the VPPC), and an increase of deformation (accompanied by exhumation and deficiency of arc plutonic magmatism) between ~465 and ~415 Ma, due to the collision of Cuyania (Precordillera) on the proto-Andean margin of Gondwana. Only from the ~415 Ma onwards (in the Devonian period) the emplacement of the postorogenic plutons like El Volcán, El Molle, Barroso, Renca, El Hornito, Las Chacras and others occurs, these represent the collapse of the Famatinian orogen produced after the collision.

Acknowledgments

Most of the data contained in this paper are part of the PhD thesis of the first author. We are grateful to Consejo Nacional de Investigaciones Científicas y Técnicas (CONICET) for the scholarships awarded to A. Morosini during his PhD studies. We would like to thank projects Nº 3-2-0114 (UNSL) and PICT 2014 Nº 0958 foncyt (Argentina), for the financial support. The authors are grateful for the thorough review of the manuscript by E. Llambías and L. Pinotti, and for the valuable suggestions performed by A.M. Sato. They are also grateful the Regional-Editor V. Ramos and Editor-in-Chief J. Kellogg.

References

Aceñolaza, F.G., Toselli, A.J., 1976. Consideraciones estratigráficas y tectónicas sobre el Paleozoico inferior del Noroeste Argentino. In: 2º Congreso Latinoamericano

de Geología, Actas, vol 2, pp. 755–764.
Aceñolaza, F.G., Toselli, A.J., 1981. Geología del Noroeste Argentino. In: Facultad Ciencias Naturales e Instituto Miguel Lillo, 1287. Universidad Nacional Tucumán, pp. 1–212. Publicación Especial.
Boynton, W.V., 1984. Cosmochemistry of the rare earth elements: meteorite studies. In: Henderson, P. (Ed.), Rare Earth Element Geochemistry. Elsevier, Amsterdam, pp. 63–114.
Brogioni, N., 1994. Petrología de la faja de rocas máficas y ultramáficas de la Sierra de San Luis, Argentina. In: 7° Congreso Geológico Chileno, Actas, vol. 2, pp. 967–971 (Concepción, Chile).
Brogioni, N., Parrini, P., Pecchioni, E., 2005. Petrología del magmatismo de arco predeformacional en el cordón del Realito y la Zona norte del Plutón La Escalerilla. Sierra de San Luis. Rev. Asoc. Geol. Argent. 60 (3), 495, 412.
Caminos, R., 1979. Sierras Pampeanas Noroccidentales. Salta, Tucumán, Catamarca, La Rioja y San Juan. In: Turner, J.C.M. (Ed.), Segundo Simposio de Geología Regional Argentina. Academia Nacional de Ciencias, Córdoba., pp. 225–291
Chapman, J.B., Ducea, M.N., DeCelles, P.G., Profeta, L., 2015. Tracking changes in crustal thickness during orogenic evolution with Sr/Y: an example from the North American Cordillera. Geology 43 (10), 919.
Chiaradia, M., 2015. Crustal thickness control on Sr/Y signatures of recent arc magmas: an Earth scale perspective. Sci. Rep. 5, 8115. http://dx.doi.org/10.1038/srep08115.
Carugno Durán, A., Ortiz Suárez, A., 2012. Metamorfitas de baja presión en la sierra de Socoscora, San Luis, y sus implicancias regionales. Rev. Asoc. Geol. Argent. 69 (2), 185–192.
Casquet, C., Baldo, E., Galindo, C., Pankhurst, R.J., Rapela, C.W., Fanning, M.C., 2014. Las "vulcanitas" de la Formación San luis (Sierra de San luis, Argentina): Nueva edad (SHRIMP) y geoquímica isotópica (Sr - Nd). In: 19º Congreso Geológico Argentino, pp. S21–S28. Córdoba.
Criado Roque, P., Mombru, C.A., Ramos, V.A., 1981. Estructura e interpretación tectónica. In: Irigoyen, M. (Ed.), Geología y recursos naturales de la Provincia de San Luis, 8° Congreso Geológico Argentino. Relatorio, pp. 155–192.
Cruciani, G., Franceschelli, M., Brogioni, N., 2011. Mineral re-equilibration and P-T path of metagabbros, Sierra de San Luis, Argentina: insights into the exhumation of a mafic-ultramafic belt. Eur. J. Mineral. 23, 591–608.
Dalla Salda, L., 1987. Basement tectonics of the southern Pampean ranges, Argentina. Tectonics 6 (3), 249–260.
Delakowitz, B., Höll, R., Hack, M., Brodtkorb, M., Stärk, H., 1991. Geological and geochemical studies of the Sierra del Morro-Oeste (San Luis Province, Argentina): meta-sediments and meta-volcanics from a probable back-arc setting. J. S. Am. Earth Sci. 4, 189–200.
Delpino, S., Dimieri, L., Bjerg, E., Kostadinoff, J., Mogessie, A., Hoinkes, G., Hauzenberger, Ch, Felfernig, A., 2001. Geometrical analysis and timing of structures on mafic-ultramafic bodies and high-grade metamorphic rocks, Sierras Grandes of San Luis, Argentina. J. S. Am. Earth Sci. 14 (1), 101–112.
Delpino, S.H., Bjerg, E.A., Ferracutti, G.R., Mogessie, A., 2007. Counterclockwise tectonometamorphic evolution of the Pringles metamorphic complex, Sierras Pampeanas of San Luis (Argentina). J. S. Am. Earth Sci. 23, 147–175.
Drobe, M., López de Luchi, M.G., Steenken, A., Frei, R., Naumann, R., Wemmer, K., Siegesmund, 2009. Provenance of the Late Proterozoic to Early Cambrian metaclastic sediments of the Sierra de San Luis (Eastern Sierras Pampeanas) and Cordillera oriental, Argentina. J. S. Am. Earth Sci. 28, 239–262.
Ducea, M.N., Otamendi, J.E., Bergantz, G., Stair, K.M., Valencia, V.A., Gehrel, G.E., 2010. Timing constraints on building an intermediate plutonic arc crustal section: U-Pb zircon geochronology of the Sierra Valle Fértil–La Huerta, Famatinian arc, Argentina. Tectonics 29, TC4002. http://dx.doi.org/10.1029/2009TC002615.
Escayola, M.P., Pimentel, M.M., Armstrong, R., 2007. Neoproterozoic backarc basin: sensitive high-resolution ion microprobe U-Pb and Sm-Nd isotopic evidence from the Eastern Pampean Ranges, Argentina. Geology 35, 495–498.
González, P., 2003. Estructura, metamorfismo y petrología del basamento ígneo-metamórfico de la Sierra de San Luis entre Nogolí y Gasparillo. Ph.D. thesis. Universidad Nacional de La Plata, p. 446 (unpublished).
González, P., Sato, A., Basei, M., Vlach, S., Llambías, E., 2002. Structure, metamorphism and age of the Pampean-Famatinian Orogenies in the Western Sierras de San Luis. In: 15° Congreso Geológico Argentino, vol. 2, pp. 51–56. El Calafate.
Gordillo, C.E., Lencinas, A.N., 1979. Sierras Pampeanas de Córdoba y San Luis. In: Turner, J.C.M. (Ed.), Segundo Simposio de Geología Regional Argentina. Academia Nacional de Ciencias, Córdoba, pp. 577–650.
Gromet, L.P., Simpson, C., 2000. Cambrian Orogeny in the Sierras Pampeanas, Argentina: Ridge Subduction or Continental Collision? Geological Society of America Abstracts with Programs, p. A-505.
Grosso Cepparo, P., Ortiz Suárez, A., Gómez Figueroa, J., 2007. Metamorfitas Las Higueras. Sierras Pampeanas de San Luis, Argentina. In: 5º Congreso Uruguayo de Geología. Montevideo. Actas 077 CD-ROM.
Irvine, T.M., Baragar, W.R., 1971. A guide to the chemical classification of common volcanic rocks. Can. J. Earth Sci. 8, 523–548.
Jordan, T.E., Allmendinger, R.W., 1986. The Sierras Pampeanas of Argentina: a modern analogue of Rocky Mountain foreland deformation. Am. J. Sci. 286 (10), 737–764.
Kilmurray, J., Dalla Salda, L.H., 1979. Caracteres estructurales y petrológicos de la región central y sur de la Sierra de San Luis. Obra del Centenario del Museo de La Plata, La Plata, Sección geológica, pp. 167–178.
Kilmurray, J., Villar, L., 1981. El basamento de la Sierra de San Luis y su petrología. In: VIII Congreso Geológico Argentino. Relatorio, pp. 33–54.
Larrovere, M.A., de los Hoyos, C.R., Toselli, A.J., Rossi, J.N., Basei, M.A.S., Belmar, M.E., 2011. High T/P evolution and metamorphic ages of the migmatitic basement of northern Sierras Pampeanas, Argentina: characterization of a mid-crustal segment of the Famatinian belt. J. S. Am. Earth Sci. 31 (2–3), 279–297.
Le Maitre, R.W., 2002. Igneous rocks. A classification and glossary of terms: recommendations of the international union of geological sciences subcommission of the Systematics of igneous rocks. In: Le Maitre, R.W., Streckeisen, A., Zanettin, B., Le Bas, M.J., Bonin, B., Bateman, P., Bellieni, G., Dudek, A., Schmid, R., Sorensen, H., Woolley, A.R. (Eds.), second ed. Cambridge University Press, Cambridge, pp. 225–236.
López de Luchi, M., 1987. Caracterización geológica y geoquímica del plutón Las Taperas y del batolito de Renca, Sierra de San Luis, República Argentina. In: X Congreso Geológico Argentino, Tucumán, Actas, vol. 3, pp. 84–87.
López de Luchi, M., Hoffmann, A., Siegesmund, S., Wemmer, K., Steenken, A., 2002. Temporal constraints on the polyphase evolution of the Sierra de San Luis. Preliminary report based on biotite and muscovite cooling ages. In: 15° Congreso Geológico Argentino, El Calafate, Actas, vol. 1, pp. 309–315.
López de Luchi, M., Siegesmund, S., Wemmer, K., Steenken, A., Naumann, R., 2007. Geochemical constraints on the petrogenesis of the Paleozoic granitoids of the Sierra de San Luis, Sierras Pampeanas, Argentina. J. S. Am. Earth Sci. 24, 138–166.
Ludwig, K.R., 2003. In: Isoplot 3.00, vol. 4. Berkeley Geochronology Center, California, pp. 0–70. Special Publication.
Llambías, E., Sato, A.M., Ortiz Suarez, A., Prozzi, C., 1998. The granitoids of the sierra de San Luis. In: Pankhurst, R.J., Rapela, C.W. (Eds.), The Proto-Andean Margin of Gondwana, vol. 142. Geological Society, London, pp. 325–341. Special Publication.
Morosini, A., 2011. El Granito La Escalerilla, Provincia de San Luis. Ph.D. thesis. Universidad Nacional de San Luis, p. 434 (unpublished).
Morosini, A., Ortiz Suárez, A., 2010. La deformación famatiniana del granito La Escalerilla, Sierra de San Luis. Rev. Asoc. Geol. Argent. 67 (4), 481–493.
Morosini, A., Ortiz Suárez, A., 2011. El metamorfismo de contacto del granito La Escalerilla en el área de La Carolina, San Luis. Rev. Asoc. Geol. Argent. 68 (2), 279–291.
Morosini, A., Ortiz Suárez, A., Ramos, G., 2009. Los Granitoides Famatinianos del sector suroccidental de la Sierra de San Luis: Clasificación y Geotermometría. Rev. Asoc. Geol. Argent. 64 (3), 253–266.
Morosini, A., Enriquez, E., Ortiz Suárez, A., Ramos, G., Carugno Durán, A., Ulacco, J., 2014. Hipótesis de extrusión vinculada a la inversión metamórfica del Complejo Metamórfico Pringles, sierra de San Luis. In: XIX Congreso Geológico Argentino, CD, pp. S21–S38. Córdoba.
Ortiz Suárez, A., 1988. El basamento de Las Aguadas, provincia de San Luis. Revista de la Asociación Argentina de Mineralogía. Petrol. Sedimentol. 19 (1–4), 13–24.
Ortiz Suárez, A., 1999. Geología y petrología del área de San Francisco del Monte de Oro, San Luis. Ph.D. thesis. Universidad Nacional de San Luis, p. 259 (unpublished).
Ortiz Suárez, A., Casquet, M.C., 2005. Inversión metamórfica en el orógeno famatiniano de la Sierra de San Luis, Argentina. Geogaceta 38, 231–234.
Ortiz Suárez, A., Prozzi, C., Llambías, E., 1992. Geología de la parte Sur de la Sierra de San Luis y granitoides asociados, Argentina. Rev. Estud. Geol. 48, 269–277. Madrid.
Ortiz Suárez, A., Morosini, A., Ulacco, H., Carugno Durán, A., 2012. Geología y geofísica del cuerpo máfico-ultramáfico Las Cañas, Provincia de San Luis. Ser. Correl. Geol. 28, 09–26.
Otamendi, J.E., Vujovich, G.I., de la Rosa, J.D., Castro, A., Tibaldi, A., Martino, R., Pinotti, L., 2009. Geology and petrology of a deep crustal zone the famatinian paleoarc, Sierras Valle Fértil – La Huerta, San Juan, Argentina. J. S. Am. Earth Sci. 27, 258–279.
Pankhurst, R.J., Rapela, C.W., Fanning, C.M., 2000. Age and origin of coeval TTG, I- and S-type granites in the Famatinian belt of NW Argentina. Trans. R. Soc. Edinb. Earth Sci. 91, 151–168.
Paterson, S.R., Ducea, M.N., 2015. Introduction to magmatic arc tempos. Elements 11, 91–98.
Patiño Douce, A.E., Beard, J.S., 1995. Dehydration melting of biotite gneiss and quartz amphibolite from 3 to 15 kbar. J. Petrol. 36, 707–738.
Peccerillo, A., Taylor, S.R., 1976. Geochemistry of Eocene calc-alkaline volcanic rocks from the Kastamonu area, Northern Turkey. Contrib. Min Petrol. 58, 63–81.
Prozzi, C., Ramos, G., 1988. La formación San Luis. Primeras Jornadas de Trabajo de Sierras Pampeanas. San Luis, Abstracts, 1.
Ramos, V.A., Cristallini, E.O., Pérez, D.J., 2002. The Pampean flat-slab of the central Andes. J. S. Am. Earth Sci. 15, 59–78.
Ramos, V.A., Martino, R.D., Otamendi, J.E., Escayola, M.P., 2014. Evolución geotectónica de las Sierras Pampeanas Orientales. In: Martino, R.D., y Guereschi, A.B. (Eds.), Geología y Recursos Naturales de la provincia de Córdoba, Asociación Geológica Argentina, 19º Congreso Geológico Argentino, vol. 1. Relatorio, Córdoba, pp. 965–977.
Rapela, C.W., Coira, B., Toselli, A., Saavedra, J., 1992. The lower Paleozoic magmatism of southwestern Gondwana and the evolution of the famatinian orogen. Int. Geol. Rev. 34 (II), 1081 l142.
Rapela, C.W., Pankhurst, R.J., Baldo, E., Casquet, C., Galindo, C., Fanning, C.M., Saavedra, J., 2001. Ordovician metamorphism in the Sierras Pampeanas: new U-Pb SHRIMP ages in central-east Valle Fértil and the Velasco Batholith. In: Revista Comunicaciones Edición Especial 3º South American Symposium on Isotope Geology. Servicio Nacional de Geología y Minería, Santiago,

pp. 616–619. Abbreviated Abstracts: 165. CD.
Rapela, C.W., Pankhurst, R.J., Casquet, C., Fanning, C.M., Baldo, E.G., González-Casado, J.M., Galindo, C., Dahlquist, J., 2007. The Río de la Plata craton and the assembly of SW Gondwana Earth. Sci. Rev. 83, 49–82.
Sato, A.M., Llambías, E., 1994. Granitoides pre-cinemáticos del sur de las Sierras de San Luis, Argentina. In: VII Congreso Geológico Chileno, Actas, vol. 2, pp. 1200–1204.
Sato, A.M., Ortiz Suárez, A., Llambías, E., Cavarozzi, C., Sánchez, V., Varela, R., Prozzi, C., 1996. Los plutones pre-oclóyicos de la Sierra de San Luis: arco magmático al inicio del ciclo famatiniano. In: XIII Congreso Geológico Argentino y III Congreso de Exploración de Hidrocarburos, Actas, vol. 5, pp. 259–272.
Sato, A.M., González, P.D., Petronilho, L.A., Llambías, E.J., Varela, R., Basei, M.A.S., 2001. Sm-Nd, Rb-Sr and K-Ar age constraints of the El Molle and Barroso plutons, western Sierra de San Luis, Argentina. In: III South American Symposium on Isotope Geology. Sociedad Geológica de Chile, Santiago, pp. 241–244. Extended Abstract Volume (CD-ROM).
Sato, A.M., Gonzáles, P., Llambías, E., 2003a. Evolución del orógeno Famatiniano en la Sierra de San Luis: magmatismo de arco, deformación y metamorfísmo de bajo a alto grado. Rev. Asoc. Geol. Argent. 58 (4), 487–504.
Sato, A.M., González, P.D., Basei, M.A., Passarelli, C.R., Tickyj, H., Ponce, J.M., 2003b. The famatinian granitoids of southwestern Sierra de San Luis, Argentina. In: IV South American Symposium on Isotope Geology, pp. 290–293. Short Papers.
Sato, A.M., González, P.D., Basei, M.A.S., Passarelli, C.R., Sato, K., Vlach, S., Varela, R., Llambías, E.J., 2004. The Famatinian orogeny of western Sierra de San Luis, Argentina. In: Simposio 40 Anos de Geocronología no Brasil, p. 83. Abstracts book.
Sato, A.M., González, P., Basei, M.A.S., 2005. Los ortogneises granodioríticos del Complejo Metamórfico Nogolí, Sierra de San Luis. In: 16° Congreso Geológico Argentino, La Plata, Actas, vol. 1, pp. 33–40.
Siegesmund, S., Steenken, A., López de Luchi, M.G., Wemmer, K., Hofmann, A., Mosch, S., 2004. The Chacras - Potrerillos batholit (Pampean ranges, Arg.): Structural evidences, emplacement and timing of the intrusion. Int. J. Earth Sci. 93, 23–43 (Geologische Rundschau).
Sims, J., Ireland, T., Camacho, A., Lyons, P., Pieters, P., Skirrow, R., Stuart-Smith, P., Miró, R., 1998. U-Pb, Th-Pb and Ar-Ar geochronology from the southern Sierras Pampeanas, Argentina: implications for the Paleozoic tectonic evolution of the western Gondwana margin. In: Pankhurst, R.J., Rapela, C.W. (Eds.), The Proto-Andean Margin of Gondwana, vol. 142. Geological Society, London, pp. 256–281. Special Publication.
Sims, J.P., Stuart-Smith, P.G., Lyons, P., Skirrow, R.G., 1997. Report on Geological and Metallogenic Maps, Sierras de San Luis and Comechingones. In: Provinces of San Luis and Córdoba", Scale 1:250,000.
Stacey, J.S., Kramers, J.D., 1975. Approximation of terrestrial lead isotope evolution by a two-stage model. Earth Planet. Sci. Lett. 26 (2), 207–221.
Steenken, A., López de Luchi, M.G., Martino, R.D., Siegesmund, S., Wemmer, K., 2005. SHRIMP dating of the El Peñón granite: a time marker at the turning point between the Pampean and Famatinian cycles within the Conlara Metamorphic Complex (Sierra de San Luis; Argentina). In: 16º Congreso Geológico Argentino, Actas, pp. 889–896 (La Plata, Buenos Aires).
Steenken, A., Siegesmund, S., Lopez de Luchi, M.G., Frei, R., Wemmer, K., 2006. Neoproterozoic to early Palaeozoic events in the Sierra de San Luis: implications for the Famatinian geodynamics in the Eastern Sierras Pampeanas (Argentina). J. Geol. Soc. 163, 965–982.
Steenken, A., Siegesmund, S., Wemmer, K., López de Luchi, M.G., 2008. Time constraints on the Famatinian and Achalian structural evolution of the basement of the Sierra de San Luis (Eastern Sierras Pampeanas, Argentina). J. S. Am. Earth Sci. 25 (3), 336–358.
Steenken, A., López de Luchi, M.G., Martínez Dopico, C., Drobe, M., Wemmer, K., Siegesmund, S., 2010. The Neoproterozoic-early Paleozoic metamorphic and magmatic evolution of the Eastern Sierras Pampeanas: an overview. Int. J. Earth Sci. 1–24. http://dx.doi.org/10.1007/s00531-010-0624-0.
Steenken, A., López de Luchi, M.G., Martínez Dopico, C., Drobe, M., Wemmer, K., Siegesmund, S., 2011. The Neoproterozoic-early Paleozoic metamorphic and magmatic evolution of the Eastern Sierras Pampeanas: an overview. In: Siegesmund, S., Basei, M., Oyhantcabal, P. (Eds.), Multiaccretional Tectonics at the Rio de La Plata Margins, pp. 465–488. Int. J. Earth Sci., vol. 100(2).
Stuart-Smith, P., Camacho, A., Sims, J., Skirrow, R., Lyons, P., Pieters, P., Black, L., Miró, R., 1999. Uranium-lead dating of félsica magmatic cycles in the southern Sierras Pampeanas, Argentina: implications for the tectonic development of the proto-Andean Gondwana margin. In: Ramos, V.A., Keppie, J.D. (Eds.), Laurentia-gondwana before Pangea, vol. 336. Geological Society of America, pp. 87–114. Special Paper.
Thomas, W., Astini, R., 1996. The Argentine Precordillera: a traveler from the Ouachita embayment of North American Laurentia. Sciences 273, 752–757.
Thompson, R.N., 1982. Magmatism of the British tertiary Volcanic Province. Scott. J. Geol. 18, 49–107.
Villaseca, C., Barbero, L., Herreros, V., 1998. A re-examination of the typology of peraluminous granite types in intracontinental orogenic belts. Trans. R. Soc. Edinb. Earth Sci. 89, 113–119.
von Gosen, W., 1998. Transpressive deformation in the southwestern part of the Sierras de San Luis (Sierras Pampeanas, Argentina). J. S. Am. Earth Sci. 11 (3), 233–264.
von Gosen, W., Prozzi, C., 1998. Structural Evolution of the Sierra de San Luis (Eastern Sierras Pampeanas, Argentina): implications for the proto-andean Margin of Gondwana. In: Pankhurst, R.J., Rapela, C.W. (Eds.), The Proto-Andean Margin of Gondwana, vol. 142. Geological Society, London, pp. 235–258. Special Publication.
von Gosen, W., Loske, W., Prozzi, C., 2002. New isotopic dating of intrusive rocks in the Sierra de San Luis (Argentina): implications for the geodinamic history of the Eastern Sierras Pampeanas. J. S. Am. Earth Sci. 15, 237–250.
Whitmeyer, S.J., Simpson, C., 2004. Regional deformation of the Sierra de San Luis, Argentina: implications for the Paleozoic development of western Gondwana. Tectonics 23, TC1005. http://dx.doi.org/10.1029/2003TC001542.
Whitney, D.L., Evans, B.W., 2010. Abbreviations for names of rock-forming minerals. Am. Mineral. 95, 185–187.